Eur. Phys. J. C (2019) 79:313
https://doi.org/10.1140/epjc/s10052-019-6788-2

THE EUROPEAN PHYSICAL JOURNAL C

Regular Article - Experimental Physics

Measurement of the top quark mass in the all-jets final state at $\sqrt{s} = 13$ TeV and combination with the lepton+jets channel

CMS Collaboration*

CERN, 1211 Geneva 23, Switzerland

Received: 26 December 2018 / Accepted: 14 March 2019

Abstract A top quark mass measurement is performed using 35.9 fb^{-1} of LHC proton–proton collision data collected with the CMS detector at $\sqrt{s} = 13$ TeV. The measurement uses the $\mathrm{t\bar{t}}$ all-jets final state. A kinematic fit is performed to reconstruct the decay of the $\mathrm{t\bar{t}}$ system and suppress the multijet background. Using the ideogram method, the top quark mass (m_t) is determined, simultaneously constraining an additional jet energy scale factor (JSF). The resulting value of $m_\mathrm{t} = 172.34 \pm 0.20\,\text{(stat+JSF)} \pm 0.70\,\text{(syst)}$ GeV is in good agreement with previous measurements. In addition, a combined measurement that uses the $\mathrm{t\bar{t}}$ lepton+jets and all-jets final states is presented, using the same mass extraction method, and provides an m_t measurement of $172.26 \pm 0.07\,\text{(stat+JSF)} \pm 0.61\,\text{(syst)}$ GeV. This is the first combined m_t extraction from the lepton+jets and all-jets channels through a single likelihood function.

1 Introduction

The top quark [1,2] is the most massive known fundamental particle and its mass m_t is an important parameter of the standard model (SM) of particle physics. Precise measurements of m_t can be used to test the internal consistency of the SM [3–5] and to search for new physical phenomena. Since the top quark dominates the higher-order corrections to the Higgs boson mass, a precise m_t determination is crucial to put constraints on the stability of the electroweak vacuum [6,7].

At the CERN LHC, top quarks are predominantly produced in quark-antiquark pairs ($\mathrm{t\bar{t}}$) through the gluon fusion process, and decay almost exclusively to a bottom quark and a W boson. Each $\mathrm{t\bar{t}}$ event can be classified through the decays of the W bosons. Events in the all-jets final state correspond to those that have both W bosons decaying further into $\mathrm{q\bar{q}'}$ pairs, while events in the lepton+jets final state have one W boson decaying to a charged lepton and a neutrino.

This paper presents a measurement of m_t obtained in the $\mathrm{t\bar{t}}$ all-jets decay channel using proton–proton (pp) collision data taken in 2016 by the CMS experiment at a center-of-mass energy of $\sqrt{s} = 13$ TeV, corresponding to an integrated luminosity of 35.9 fb^{-1}. The two bottom quarks and the four light quarks from the $\mathrm{t\bar{t}}$ decay are all required to be physically separated in the laboratory frame of reference, and the nominal experimental signature is therefore characterized by six jets in the detector.

Although this final state provides the largest branching fraction of all $\mathrm{t\bar{t}}$ decays, this measurement of m_t is particularly challenging, because of the large background from multijet production. A kinematic fit of the decay products to the $\mathrm{t\bar{t}}$ hypothesis is therefore employed to separate signal from background events.

The value of m_t is extracted using the ideogram method [8,9], which is based on a likelihood function that depends either just on the mass parameter m_t, or on m_t combined with an additional jet energy scale factor (JSF). In the second case, the invariant mass of the two jets associated with the $\mathrm{W} \to \mathrm{q\bar{q}'}$ decay serves as an observable to directly estimate the JSF.

Previous measurements in this decay channel have been performed by Tevatron and LHC experiments at lower center-of-mass energies [10–14]. The most precise one of these has been obtained by CMS at $\sqrt{s} = 8$ TeV, resulting in a mass of $m_\mathrm{t} = 172.32 \pm 0.25\,\text{(stat+JSF)} \pm 0.59\,\text{(syst)}$ GeV. Combining the results of several measurements using different final states at $\sqrt{s} = 7$ and 8 TeV, ATLAS and CMS reported values of $m_\mathrm{t} = 172.69 \pm 0.48$ GeV [15] and 172.44 ± 0.48 GeV [12], respectively, while a value of $m_\mathrm{t} = 174.30 \pm 0.65$ GeV was obtained by combining the Tevatron results [16].

The top quark mass has been measured for the first time with pp data at $\sqrt{s} = 13$ TeV, using the lepton+jets channel [17], yielding a value of $m_\mathrm{t} = 172.25 \pm 0.08\,\text{(stat+JSF)} \pm 0.62\,\text{(syst)}$ GeV. A measurement using both $\mathrm{t\bar{t}}$ all-jets and lepton+jets events is presented here. This is possible since the two measurements use the same mass extraction method, so a single likelihood can be used, rather than just combining

* e-mail: cms-publication-committee-chair@cern.ch

Published online: 06 April 2019

the two results statistically. With this approach, no assumptions on correlations between different uncertainties of the measurements have to be made. This is the first report of a combined m_t measurement in the lepton+jets and all-jets final states using a single likelihood function.

2 The CMS detector and event reconstruction

The central feature of the CMS apparatus is a superconducting solenoid of 6 m internal diameter, providing a magnetic field of 3.8 T. Within the solenoid volume are a silicon pixel and strip tracker, a lead tungstate crystal electromagnetic calorimeter (ECAL), and a brass and scintillator hadron calorimeter (HCAL), each composed of a barrel and two endcap sections. Forward calorimeters extend the pseudorapidity (η) coverage provided by the barrel and endcap detectors. Muons are detected in gas-ionization chambers embedded in the steel flux-return yoke outside the solenoid.

Events of interest are selected using a two-tiered trigger system [18]. The first level, composed of custom hardware processors, uses information from the calorimeters and muon detectors to select events within a time interval of 4 μs, resulting in a trigger rate of around 100 kHz. The second level, known as the high-level trigger (HLT), consists of a farm of processors running a version of the full event reconstruction software optimized for fast processing, and reduces the event rate to around 1 kHz before data storage.

The particle-flow (PF) algorithm [19] aims to reconstruct and identify each individual particle in an event, with an optimized combination of information from the various elements of the CMS detector. The energy of photons is obtained from the ECAL measurement. The energy of electrons is determined from a combination of the electron momentum at the primary interaction vertex as determined by the tracker, the energy of the corresponding ECAL cluster, and the energy sum of all bremsstrahlung photons spatially compatible with originating from the electron track. The energy of muons is obtained from the curvature of the corresponding track. The energy of charged hadrons is determined from a combination of their momentum measured in the tracker and the matching ECAL and HCAL energy deposits, corrected for zero-suppression effects and for the response function of the calorimeters to hadronic showers. Finally, the energy of neutral hadrons is obtained from the corresponding corrected ECAL and HCAL energy.

The reconstructed vertex with the largest value of summed physics-object p_T^2 is taken to be the primary proton–proton interaction vertex. The physics objects are the jets, clustered using the jet finding algorithm [20,21] with the tracks assigned to the vertex as inputs, and the associated missing transverse momentum, taken as the negative vector sum of the transverse momentum p_T of those jets.

Jets are clustered from PF objects using the anti-k_T algorithm with a distance parameter of 0.4 [20–22]. Jet momentum is determined as the vectorial sum of all particle momenta in the jet, and is found from simulation to be within 5–10% of the true momentum over the whole p_T spectrum and detector acceptance. Additional proton–proton interactions within the same or nearby bunch crossings (pileup) can contribute additional tracks and calorimetric energy depositions to the jet momentum. To mitigate this effect, tracks identified to be originating from pileup vertices are discarded, and an offset correction is applied to correct for remaining contributions from neutral hadrons. Jet energy corrections (JECs) are derived from simulation to bring the measured response of jets to that of particle level jets on average. In situ measurements of the momentum balance in dijet, photon+jet, Z+jet, and multijet events are used to account for any residual differences in the jet energy scale in data and simulation [23]. Additional selection criteria are applied to each jet to remove jets dominated by anomalous contributions from various subdetector components or reconstruction failures [24].

A more detailed description of the CMS detector, together with a definition of the coordinate system used and the relevant kinematic variables, can be found in Ref. [25].

3 Event selection and simulation

Only jets with $p_T > 30$ GeV reconstructed within $|\eta| < 2.4$ are used in the analysis. For the identification of jets originating from the hadronization of b quarks, the combined secondary vertex algorithm (CSVv2) b tagger is used [26]. The chosen working point provides an identification efficiency of approximately 50% with a probability of misidentifying a u/d/s quark jet or gluon jet as being a bottom jet of approximately 0.1%, and a misidentification probability for c quark jets of 2%. The hadronic activity, used for the event selection, is defined as the scalar p_T sum of all jets in the event,

$$H_T \equiv \sum_{\text{jets}} p_T.$$

Data events are selected using an HLT that requires the presence of at least six PF jets with $p_T > 40$ GeV and $H_T > 450$ GeV. Additionally, the HLT requires at least one jet to be b tagged.

In the offline selection, an event must contain a well reconstructed vertex localized within 24 cm in the z direction and 2 cm in the x–y plane around the nominal interaction point. Selected events are required to contain at least six jets, at least two of which have to be tagged as b jets. The sixth jet (jet_6), ordered in decreasing p_T, must fulfill $p_T(\text{jet}_6) > 40$ GeV, and $H_T > 450$ GeV is required. The two b jets must be separated in $\Delta R = \sqrt{\Delta\phi^2 + \Delta\eta^2}$ by $\Delta R(\text{b}\bar{\text{b}}) > 2.0$.

The $\mathrm{t\bar{t}}$ signal is simulated at an m_{t} of 172.5 GeV using the POWHEG v2 [27–29] matrix-element (ME) generator in next-to-leading order (NLO) perturbative quantum chromodynamics (QCD). For the parton distribution functions (PDFs), the NNPDF3.0 NLO set [30] is used with the strong coupling constant value of $\alpha_S = 0.118$. This is one of the first PDF sets to include the total $\mathrm{t\bar{t}}$ cross section measurements from ATLAS and CMS at $\sqrt{s} = 7$ and 8 TeV as input. The parton shower (PS) and hadronization are handled by PYTHIA 8.219 [31] using the CUETP8M2T4 tune [32,33] and GEANT4 is used to simulate the response of the CMS detector [34]. The simulated signal sample is normalized to the integrated luminosity of the data sample using a cross section of $\sigma_{\mathrm{t\bar{t}}} = 832$ pb, calculated at next-to-next-to-leading order in QCD including resummation of next-to-next-to-leading logarithmic soft gluon terms [35]. In addition to the default sample, six other samples are used assuming top quark masses of 166.5, 169.5, 171.5, 173.5, 175.5, and 178.5 GeV, and using the corresponding cross sections.

For simulated events, a trigger emulation is used. The residual differences in the trigger efficiency between data and simulation are corrected by applying scale factors to the simulated events. These are obtained by measuring the trigger efficiency with respect to a reference H_{T} trigger for both data and simulation. The parameterized ratio as a function of $p_{\mathrm{T}}(\mathrm{jet}_6)$ and H_{T} is used to reweight the simulated events. Additional pp collisions are included in the simulated events. These are weighted to match the pileup distribution in data. Finally, corrections to the jet energy scale and resolution, as well as to the b tagging efficiency and misidentification rate, are applied to the simulated events.

4 Kinematic fit and background estimation

To improve the resolution of the top quark mass and decrease the background contribution, a kinematic fit is applied. It exploits the known topology of the signal events, i.e., pair production of a heavy particle and antiparticle, each decaying to Wb with $\mathrm{W} \to \mathrm{q\bar{q}'}$. The three-momenta of the jets are fitted such that

$$\chi^2 = \sum_{j \in \mathrm{jets}} \left[\frac{\left(p_{\mathrm{T}\,j}^{\mathrm{reco}} - p_{\mathrm{T}\,j}^{\mathrm{fit}}\right)^2}{\sigma_{p_{\mathrm{T}}\,j}^2} + \frac{\left(\eta_j^{\mathrm{reco}} - \eta_j^{\mathrm{fit}}\right)^2}{\sigma_{\eta_j}^2} + \frac{\left(\phi_j^{\mathrm{reco}} - \phi_j^{\mathrm{fit}}\right)^2}{\sigma_{\phi_j}^2} \right]$$

is minimized, where all jets assigned to the $\mathrm{t\bar{t}}$ decay system are considered. The labels "reco" and "fit" denote the components of the originally reconstructed and the fitted jets, respectively, and the corresponding resolutions are labeled σ_X. The minimization is performed, constraining the invariant mass of the jets assigned to each W boson decay to $m_{\mathrm{W}} = 80.4$ GeV. As an additional constraint, the two top quark candidates are required to have equal invariant masses.

All possible parton-jet assignments are tested using the leading six jets in the event, but only b-tagged jets are used as b candidates and equivalent choices (e.g., swapping the two jets originating from one W boson) are not considered separately. Of the remaining 12 possibilities, only the assignment yielding the smallest χ^2 is used in the following. The χ^2 value can be used as a goodness-of-fit (gof) measure. For three degrees of freedom, it is translated into a p-value of

$$P_{\mathrm{gof}} \equiv 1 - \mathrm{erf}\left(\sqrt{\frac{\chi^2}{2}}\right) + \sqrt{\frac{2\chi^2}{\pi}}\mathrm{e}^{-\chi^2/2}.$$

Events are required to fulfill $P_{\mathrm{gof}} > 0.1$ for the best assignment.

In simulation, event generator information can be used to validate the assignment of the reconstructed jets to the top quark decay products. Events are classified accordingly as *correct* or *wrong* permutations. A parton-jet assignment is considered correct if the jets can be matched unambiguously to the right partons within $\Delta R < 0.3$. Wrong permutations can occur because of a wrong parton-jet assignment, yielding the smallest χ^2 or jets being out of acceptance, not being reconstructed, or failing the identification requirements.

The P_{gof} distribution is displayed in Fig. 1 (right). Requiring $P_{\mathrm{gof}} > 0.1$ increases the fraction of correct permutations from 6 to 51%. The fitted top quark mass ($m_{\mathrm{t}}^{\mathrm{fit}}$) is calculated as the invariant mass of the corresponding jets returned by the kinematic fit. Compared to the mass calculated from the originally reconstructed jets, the mass resolution is improved from 14.0 to 8.8 GeV for the correct parton-jet assignments, where, in both cases, the same events passing the $P_{\mathrm{gof}} > 0.1$ requirement are used.

The $\Delta R(\mathrm{b\bar{b}}) > 2.0$ and $P_{\mathrm{gof}} > 0.1$ requirements greatly reduce the background from QCD multijet production from approximately 80 to 25%, but a significant number of multijet events enters the signal selection owing to the large production cross section of that background contribution. These events can fulfill the goodness-of-fit criterion because of combinatorial chance, but not because of an underlying decay topology. Therefore, it is assumed that b jets can be exchanged with light-flavor jets for the estimation of the background from data, because the probability for mimicking the $\mathrm{t\bar{t}}$ topology is the same.

For the background estimation, the same selection as for the signal is applied, as described above, but instead of requiring two b-tagged jets, events with exactly zero b-tagged jets are used. For this veto, a very loose working point is used for

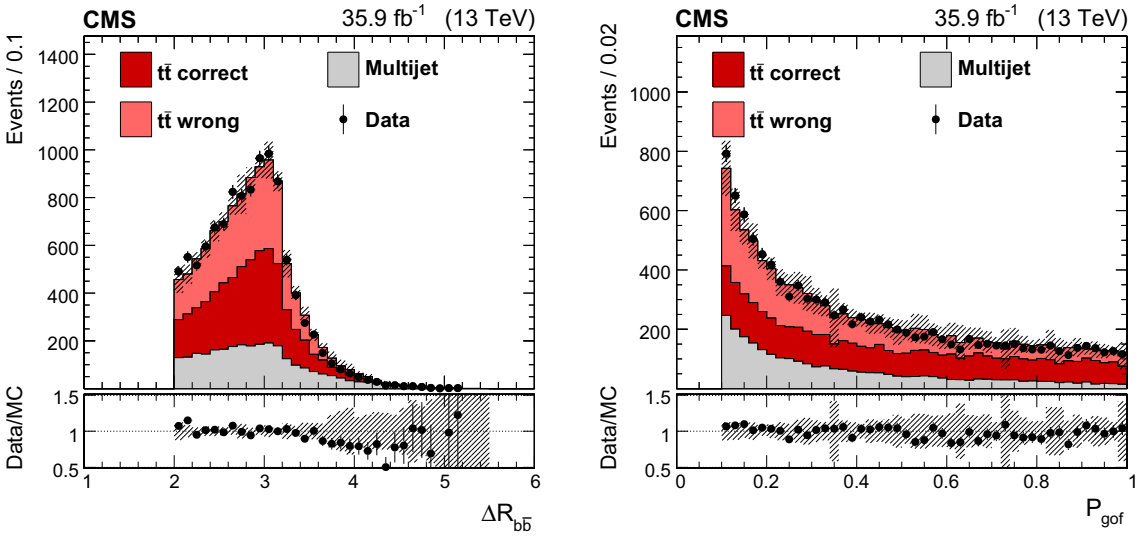

Fig. 1 The $\Delta R(\mathrm{b\bar{b}})$ (left) and P_{gof} (right) distributions of data compared to simulated signal and the multijet background estimate. For each event, the parton-jet assignment yielding the smallest χ^2 in the kinematic fit is used. The simulated signal events are classified as correct or wrong assignments and displayed separately, and the distributions are normalized to the integrated luminosity. For the background estimate, the total normalization is given by the difference of observed data events and expected signal events. The hashed bands represent the total uncertainty in the complete prediction. The lower panels show the ratio of data and prediction

the b tagger, to suppress contamination from $\mathrm{t\bar{t}}$ events in this QCD-enriched sample. A prescaled trigger similar to the signal trigger is used for this selection, which does not require the presence of b jets. The kinematic fit is applied as before, but here any of the six light-flavor jets can be assigned to the partons originating from the W decays, as well as to the partons serving as b quarks, leading to 90 possible permutations that have to be evaluated. This method allows one to determine the kinematic distributions of the background, but the normalization is unknown. In all plots, the background is normalized to the difference of the number of data events and the number of expected signal events. This data sample contains approximately five times the number of expected background events, so it provides good statistical precision.

The final selected data set consists of 10,799 events with a signal purity of 75%. Figure 1 shows the distributions of the separation of the two b jets $\Delta R(\mathrm{b\bar{b}})$ and the quantity P_{gof} in data, compared to the background estimate and $\mathrm{t\bar{t}}$ simulation. For the $\mathrm{t\bar{t}}$ signal, correct and wrong parton-jet assignments are shown separately. The corresponding distributions of $m_{\mathrm{t}}^{\mathrm{fit}}$ and the reconstructed W boson mass $m_{\mathrm{W}}^{\mathrm{reco}}$, calculated from the originally reconstructed jets, are shown in Fig. 2. These two quantities are used in the top quark mass extraction described in the following section.

5 Ideogram method

For the extraction of m_{t}, the ideogram method is used [8,9]. Simultaneously, a JSF is determined that is used in addition to the standard CMS jet energy calibration [12] to reduce the corresponding systematic uncertainty. The distributions of $m_{\mathrm{t}}^{\mathrm{fit}}$ obtained from the kinematic fit and $m_{\mathrm{W}}^{\mathrm{reco}}$ are used in a combined fit. For $m_{\mathrm{W}}^{\mathrm{reco}}$, the average mass of the two W bosons in an event is used.

The likelihood

$$\begin{aligned}\mathcal{L}\left(m_{\mathrm{t}}, \mathrm{JSF}\right) &= P\left(\mathrm{sample}|m_{\mathrm{t}}, \mathrm{JSF}\right)\\ &= \prod_{\mathrm{events}} P\left(\mathrm{event}|m_{\mathrm{t}}, \mathrm{JSF}\right)\\ &= \prod_{\mathrm{events}} P\left(m_{\mathrm{t}}^{\mathrm{fit}}, m_{\mathrm{W}}^{\mathrm{reco}}|m_{\mathrm{t}}, \mathrm{JSF}\right)\end{aligned}$$

is maximized, yielding the best fit values for m_{t} and JSF. A prior probability for the JSF can be incorporated by maximizing

$$P\left(\mathrm{JSF}\right) P\left(\mathrm{sample}|m_{\mathrm{t}}, \mathrm{JSF}\right)$$

instead. Treating $m_{\mathrm{t}}^{\mathrm{fit}}$ and $m_{\mathrm{W}}^{\mathrm{reco}}$ as uncorrelated, as verified using simulated events, the probability $P\left(m_{\mathrm{t}}^{\mathrm{fit}}, m_{\mathrm{W}}^{\mathrm{reco}}|m_{\mathrm{t}}, \mathrm{JSF}\right)$ factorizes into

$$\begin{aligned}&P\left(m_{\mathrm{t}}^{\mathrm{fit}}, m_{\mathrm{W}}^{\mathrm{reco}}|m_{\mathrm{t}}, \mathrm{JSF}\right)\\ &= f_{\mathrm{sig}} P\left(m_{\mathrm{t}}^{\mathrm{fit}}, m_{\mathrm{W}}^{\mathrm{reco}}|m_{\mathrm{t}}, \mathrm{JSF}\right)\\ &\quad + \left(1 - f_{\mathrm{sig}}\right) P_{\mathrm{bkg}}\left(m_{\mathrm{t}}^{\mathrm{fit}}, m_{\mathrm{W}}^{\mathrm{reco}}\right)\\ &= f_{\mathrm{sig}} \sum_j f_j P_j\left(m_{\mathrm{t}}^{\mathrm{fit}}|m_{\mathrm{t}}, \mathrm{JSF}\right) P_j\left(m_{\mathrm{W}}^{\mathrm{reco}}|m_{\mathrm{t}}, \mathrm{JSF}\right)\\ &\quad + \left(1 - f_{\mathrm{sig}}\right) P_{\mathrm{bkg}}\left(m_{\mathrm{t}}^{\mathrm{fit}}\right) P_{\mathrm{bkg}}\left(m_{\mathrm{W}}^{\mathrm{reco}}\right),\end{aligned}$$

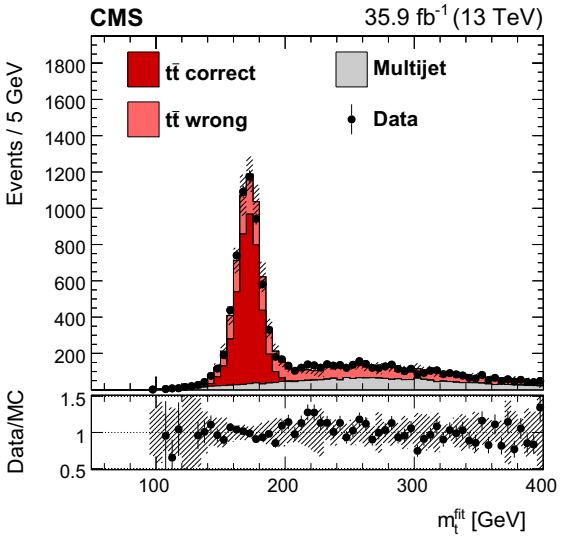

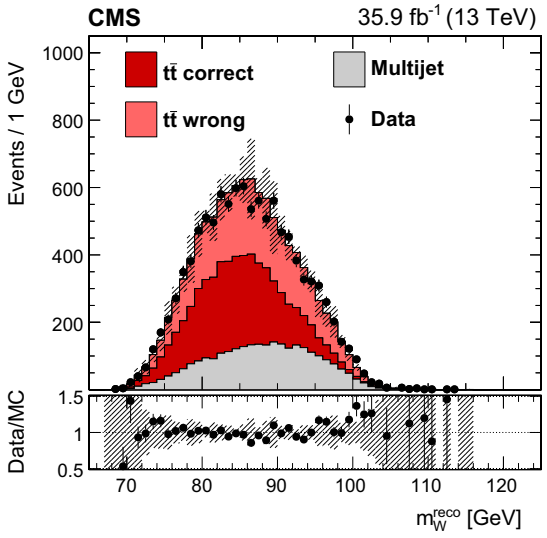

Fig. 2 The fitted top quark mass (left) and reconstructed W boson mass (right) distributions of data compared to simulated signal and the multijet background estimate. The shown reconstructed W boson mass is the average mass of the two W bosons in the event. For each event, the parton-jet assignment yielding the smallest χ^2 in the kinematic fit is used. The simulated signal events are classified as correct or wrong assignments and displayed separately, and the distributions are normalized to the integrated luminosity. For the background estimate, the total normalization is given by the difference of observed data events and expected signal events. The hashed bands represent the total uncertainty in the prediction. The lower panels show the ratio of data and prediction

where f_j with $j \in \{\text{correct, wrong}\}$ is the relative fraction of the different permutation cases and f_{sig} is the signal fraction.

The probability densities $P_j\left(m_{\text{t}}^{\text{fit}}|m_{\text{t}}, \text{JSF}\right)$ and $P_j\left(m_{\text{W}}^{\text{reco}}|m_{\text{t}}, \text{JSF}\right)$ for the signal are described by analytic functions parametrized in m_{t} and JSF. For the determination of the parameters, a simultaneous fit to simulated samples for seven different generated top quark masses $m_{\text{t}}^{\text{gen}}$ and five different input JSF values is used. The background shape is described by a spline interpolation as a function of $m_{\text{t}}^{\text{fit}}$ and $m_{\text{W}}^{\text{reco}}$, but independent of the model parameters m_{t} and JSF.

Three variations of a maximum likelihood fit are performed to extract the top quark mass. In the one-dimensional (1D) analysis, the JSF is fixed to unity (corresponding to a Dirac delta function for the prior probability), i.e., the standard CMS jet energy calibration. For the two-dimensional (2D) analysis, the JSF is a free parameter in the maximum likelihood fit, making possible a compensation of part of the systematic uncertainties. The signal fraction and correct permutation fraction are free parameters in both cases. The third (hybrid) method is a weighted combination of both approaches, corresponding to a measurement with a Gaussian constraint on the JSF around unity. In the limit of an infinitely narrow JSF constraint, the hybrid method is identical to the 1D method, while for an infinitely broad prior probability distribution, the 2D method is recovered. The width of the Gaussian constraint in the hybrid method is optimized to yield the smallest total uncertainty.

To calibrate the mass extraction method, pseudo-experiments are performed for the seven different generated values of $m_{\text{t}}^{\text{gen}}$ and three input JSF values (0.98, 1.00, and 1.02). The extracted m_{t} and JSF values are compared to the input values and the residual slopes in $m_{\text{t}}^{\text{gen}}$ and JSF are used as calibration. The residual biases after the calibration are shown in Fig. 3 for pseudo-experiments with different JSF

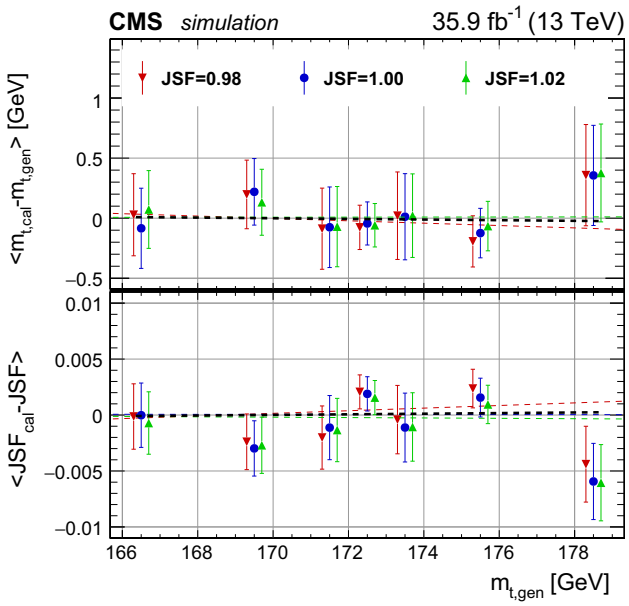

Fig. 3 Difference between extracted and generated top quark masses (upper panel) and JSFs (lower panel) for different input masses and JSFs after the calibration in the all-jets channel. The values are extracted using the 2D method

and $m_{\mathrm{t}}^{\mathrm{gen}}$ values. As expected, neither a significant residual offset nor a slope are observed after the calibration procedure.

6 Systematic uncertainties

A summary of the systematic uncertainty sources is shown in Table 1. The corresponding values are obtained from pseudo-experiments, using Monte Carlo (MC) signal samples with variations of the individual systematic uncertainty sources. In the following, details for the determination of the most important uncertainties are given. Most systematic uncertainty sources are shifted by ± 1 standard deviation, and the absolute value of the largest resulting shifts in m_{t} and JSF are quoted as systematic uncertainties for the measurement.

Table 1 List of systematic uncertainties for the all-jets channel. The signs of the shifts ($\delta x = x_{\mathrm{variation}} - x_{\mathrm{nominal}}$) correspond to the $+1$ standard deviation variation of the systematic uncertainty source. For linear sums of the uncertainty groups, the relative signs have been considered. Shifts determined using dedicated samples for the systematic variation are displayed with the corresponding statistical uncertainty

	2D		1D	Hybrid	
	$\delta m_{\mathrm{t}}^{\mathrm{2D}}$ [GeV]	$\delta \mathrm{JSF}^{\mathrm{2D}}$ [%]	$\delta m_{\mathrm{t}}^{\mathrm{1D}}$ [GeV]	$\delta m_{\mathrm{t}}^{\mathrm{hyb}}$ [GeV]	$\delta \mathrm{JSF}^{\mathrm{hyb}}$ [%]
Experimental uncertainties					
Method calibration	0.06	0.2	0.06	0.06	0.2
JEC (quad. sum)	0.18	0.3	0.73	0.15	0.2
Intercalibration	-0.04	-0.1	$+0.12$	-0.04	-0.1
MPFInSitu	-0.03	0.0	$+0.22$	$+0.08$	$+0.1$
Uncorrelated	-0.17	-0.3	$+0.69$	$+0.12$	$+0.2$
Jet energy resolution	-0.09	$+0.2$	$+0.09$	-0.04	$+0.1$
b tagging	0.02	0.0	0.01	0.02	0.0
Pileup	-0.06	$+0.1$	0.00	-0.04	$+0.1$
Background	0.10	0.1	0.03	0.07	0.1
Trigger	$+0.04$	-0.1	-0.04	$+0.02$	-0.1
Modeling uncertainties					
JEC flavor (linear sum)	-0.35	$+0.1$	-0.31	-0.34	0.0
Light quarks (uds)	$+0.10$	-0.1	-0.01	$+0.07$	-0.1
Charm	$+0.03$	0.0	-0.01	$+0.02$	0.0
Bottom	-0.29	0.0	-0.29	-0.29	0.0
Gluon	-0.19	$+0.2$	$+0.03$	-0.13	$+0.2$
b jet modeling (quad. sum)	0.09	0.0	0.09	0.09	0.0
b frag. Bowler–Lund	-0.07	0.0	-0.07	-0.07	0.0
b frag. Peterson	-0.05	0.0	-0.04	-0.05	0.0
Semileptonic b hadron decays	-0.03	0.0	-0.03	-0.03	0.0
PDF	0.01	0.0	0.01	0.01	0.0
Ren. and fact. scales	0.05	0.0	0.04	0.04	0.0
ME/PS matching	$+0.32 \pm 0.20$	-0.3	-0.05 ± 0.14	$+0.24 \pm 0.18$	-0.2
ISR PS scale	$+0.17 \pm 0.17$	-0.2	$+0.13 \pm 0.12$	$+0.12 \pm 0.14$	-0.1
FSR PS scale	$+0.22 \pm 0.12$	-0.2	$+0.11 \pm 0.08$	$+0.18 \pm 0.11$	-0.1
Top quark p_{T}	$+0.03$	0.0	$+0.02$	$+0.03$	0.0
Underlying event	$+0.16 \pm 0.19$	-0.3	-0.07 ± 0.14	$+0.10 \pm 0.17$	-0.2
Early resonance decays	$+0.02 \pm 0.28$	$+0.4$	$+0.38 \pm 0.19$	$+0.13 \pm 0.24$	$+0.3$
CR modeling (max. shift)	$+0.41 \pm 0.29$	-0.4	-0.43 ± 0.20	-0.36 ± 0.25	-0.3
"gluon move" (ERD on)	$+0.41 \pm 0.29$	-0.4	$+0.10 \pm 0.20$	$+0.32 \pm 0.25$	-0.3
"QCD inspired" (ERD on)	-0.32 ± 0.29	-0.1	-0.43 ± 0.20	-0.36 ± 0.25	-0.1
Total systematic	0.81	0.9	1.03	0.70	0.7
Statistical (expected)	0.21	0.2	0.16	0.20	0.1
Total (expected)	0.83	0.9	1.04	0.72	0.7

For some uncertainties, different models are compared, and are described individually. The maximum of the statistical uncertainty on the observed shift and the shift itself is used as the systematic uncertainty.

- *Method calibration* The quadratic sum of the statistical uncertainty and the residual bias of the calibration curve (shown in Fig. 3) after the calibration is used as the systematic uncertainty.
- *JECs* Jet energies are scaled up and down according to the p_{T}- and η-dependent data/simulation uncertainties [23]. The correlation groups (called Intercalibration, MPFInSitu, and Uncorrelated) follow the recommendations documented in Ref. [36].
- *Jet energy resolution* Since the jet energy resolution measured in data is worse than in simulation, the simulation is modified to correct for the difference [23]. The jet energy resolution in the simulation is varied up and down within the uncertainty.
- b *tagging* The p_{T}-dependent uncertainty of the b tagging efficiencies and misidentification rates of the CSVv2 b tagger [26] are taken into account by reweighting the simulated events accordingly.
- *Pileup* To estimate the uncertainty in the determination of the number of pileup events and the reweighting procedure, the inelastic proton–proton cross section [37] used in the determination is varied by $\pm 4.6\%$.
- *Background* An uncertainty in the background prediction is obtained by applying the method to simulation and comparing the obtained estimate to the direct simulation, i.e., generated QCD multijet events passing the signal selection. A linear fit to the ratio is consistent with a constant value of unity. The slope is varied up and down within its uncertainty and used to reweight the events used for the determination of the background probability density function.
- *Trigger* To estimate the uncertainty in the trigger selection, the data/simulation scale factor described in Sect. 3 is omitted. Additionally, a base trigger requiring the presence of one muon is used to obtain the correction factor. The maximum of the observed shifts with respect to the nominal correction is quoted as an uncertainty.
- *JEC flavor* The difference between Lund string fragmentation and cluster fragmentation is evaluated comparing PYTHIA 6.422 [38] and HERWIG++ 2.4 [39]. The jet energy response is compared separately for each jet flavor [23]. Uncertainties for jets from different quark flavors and gluons are added linearly, which takes into account possible differences between the measured JSF, which is mainly sensitive to light quarks and gluons, and the b jet energy scale.
- b *jet modeling* The uncertainty associated with the fragmentation of b quarks is split into three components. The Bowler–Lund fragmentation function is varied within its uncertainties as determined by the ALEPH and DELPHI Collaborations [40,41]. As an alternative model of the fragmentation into b hadrons, the Peterson fragmentation function is used and the difference obtained relative to the Bowler–Lund fragmentation function is assigned as an uncertainty. The third uncertainty source taken into account is the semileptonic b hadron branching fraction, which is varied by -0.45% and $+0.77\%$, motivated by measurements of $\mathrm{B}^0/\mathrm{B}^+$ decays and their corresponding uncertainties [42].
- *PDF* The 100 PDF replicas of the NNPDF3.0 NLO ($\alpha_S = 0.118$) set are used to repeat the analysis [30]. The variance of the results is used to determine the PDF uncertainty. In addition, the α_S value is changed to 0.117 and 0.119. The maximum of the PDF uncertainty and the α_S variations is quoted as uncertainty.
- *Renormalization and factorization scales* The renormalization and factorization scales for the ME calculation are varied. Both are multiplied independently from each other, and simultaneously by factors of 0.5 and 2 with respect to the default values. This is achieved by appropriately reweighting simulated events. The quoted uncertainty corresponds to the envelope of the resulting shifts.
- *ME/PS matching* The matching of the POWHEG ME calculations to the PYTHIA PS is varied by shifting the parameter $h_{\mathrm{damp}} = 1.58^{+0.66}_{-0.59}$ [33] within the uncertainties. The jet response $p_{\mathrm{T}}^{\mathrm{reco}}/p_{\mathrm{T}}^{\mathrm{gen}}$ as a function of $p_{\mathrm{T}}^{\mathrm{gen}}$ is rescaled in the variation samples to reproduce the response observed in the default sample.
- *ISR PS scale* For initial-state radiation (ISR), the PS scale is varied in PYTHIA. The ISR PS scale is multiplied by factors of 2 and 0.5 in dedicated MC samples.
- *FSR PS scale* The PS scale used for final-state radiation (FSR) is scaled up by $\sqrt{2}$ and down by $1/\sqrt{2}$ [32], affecting the fragmentation and hadronization, as well additional jet emission. The jet response is rescaled in the variation samples to reproduce the response observed in the default sample.
- *Top quark* p_{T} Recent calculations suggest that the top quark p_{T} spectrum is strongly affected by next-to-next-to-leading-order effects [43]. The p_{T} of the top quark in simulation is varied to match the distribution measured by CMS [44,45] and its impact on the m_{t} measurement is quoted as a systematic uncertainty.
- *Underlying event* Measurements of the underlying event have been used to tune PYTHIA parameters describing nonperturbative QCD effects [32,33]. The parameters of the tune are varied within their uncertainties.
- *Early resonance decays* Modeling of color reconnection (CR) introduces systematic uncertainties which are estimated by comparing different CR models and settings.

In the default sample, the top quark decay products are not included in the CR process. This setting is compared to the case of including the decay products by enabling early resonance decays (ERD) in PYTHIA 8.

- *CR modeling* In addition to the default model used in PYTHIA 8, two alternative CR models are used, namely a model with string formation beyond leading color ("QCD inspired") [46] and a model allowing the gluons to be moved to another string ("gluon move") [47]. Underlying event measurements are used to tune the parameters of all models [32,33]. The largest shifts induced by the variations are assigned as the CR uncertainty.
  This approach, as well as the ERD variation, is new relative to the Run 1 results at $\sqrt{s} = 7$ and 8 TeV, because these CR models have become only recently available in PYTHIA 8. The new models were first used to evaluate the m_{t} uncertainty due to CR in Ref. [17]. Like in this analysis, the same increase in systematic uncertainty with respect to the Run 1 result has been observed.

A summary of the systematic uncertainties described above is given in Table 1. In Ref. [17], an ME generator uncertainty has been considered: Instead of using POWHEG v2 as ME generator, the MADGRAPH5_aMC@NLO 2.2.2 generator with the FxFx matching scheme is used [48,49]. The difference between the results obtained with the two generators is $\delta m_{\mathrm{t}}^{\mathrm{hyb}} = +0.31 \pm 0.52$ for the hybrid method in the all-jets channel. However, this is not significant because of the insufficient statistical precision of the available MADGRAPH5_aMC@NLO sample. Since the radiation after the top quark decay is described by PYTHIA, no significant impact of the ME generator choice is expected beyond the variation of the PS scales and matching. Therefore, no ME generator uncertainty is considered in the total uncertainty of the measurement, but the number is just quoted here as a cross-check.

7 Results

For the 2D fit using the 10 799 $\mathrm{t\bar{t}}$ all-jets candidate events, the extracted parameters are

$$m_{\mathrm{t}}^{\mathrm{2D}} = 172.43 \pm 0.22\,(\mathrm{stat+JSF}) \pm 0.81\,(\mathrm{syst})\,\mathrm{GeV}\ \text{and}$$
$$\mathrm{JSF}^{\mathrm{2D}} = 0.996 \pm 0.002\,(\mathrm{stat}) \pm 0.009\,(\mathrm{syst}).$$

The corresponding 1D and hybrid fits yield instead

$$m_{\mathrm{t}}^{\mathrm{1D}} = 172.13 \pm 0.17\,(\mathrm{stat}) \pm 1.03\,(\mathrm{syst})\,\mathrm{GeV},$$
$$m_{\mathrm{t}}^{\mathrm{hyb}} = 172.34 \pm 0.20\,(\mathrm{stat+JSF}) \pm 0.70\,(\mathrm{syst})\,\mathrm{GeV},\ \text{and}$$
$$\mathrm{JSF}^{\mathrm{hyb}} = 0.997 \pm 0.002\,(\mathrm{stat}) \pm 0.007\,(\mathrm{syst}).$$

In all cases the fitted values for the fraction of correct assignments, as well as the background fraction, are in agreement with the values expected from simulation. The hybrid measurement of $172.34 \pm 0.20\,(\mathrm{stat+JSF}) \pm 0.43\,(\mathrm{CR+ERD}) \pm 0.55\,(\mathrm{syst})$ GeV is the main result of this analysis, since it is constructed to provide the smallest uncertainty. The color reconnection and early resonance decay parts are separated from the rest of the systematic uncertainties. Because of the larger data sample used in this analysis, the statistical uncertainty is reduced with respect to the result of $m_{\mathrm{t}} = 172.32 \pm 0.25\,(\mathrm{stat+JSF}) \pm 0.59\,(\mathrm{syst})$ GeV obtained at $\sqrt{s} = 8$ TeV. The new result is in good agreement with the value measured at $\sqrt{s} = 8$ TeV, where a leading-order $\mathrm{t\bar{t}}$ simulation has been employed to calibrate the measurement, whereas an NLO simulation has been used here. The systematic uncertainty is increased with respect to the Run 1 result, because a broader set of CR models has been compared, which have become available in PYTHIA 8.

8 Combined measurement with the lepton+jets final state

This measurement is combined with the lepton+jets final state, where only electrons and muons are explicitly considered as leptons, while tau leptons enter the selection only when they decay leptonically. The corresponding analysis for the lepton+jets final state is described in Ref. [17]. All selection and analysis steps are kept unchanged. Since the same method for the mass extraction is used, a combination with the all-jets channel at the likelihood level is possible.

The total likelihood $\mathcal{L}$ is constructed from the single-channel likelihoods $\mathcal{L}_i$,

$$\mathcal{L}(m_{\mathrm{t}}, \mathrm{JSF}) = \mathcal{L}_{\mathrm{A}}(m_{\mathrm{t}}, \mathrm{JSF})\mathcal{L}_{\mathrm{L}}(m_{\mathrm{t}}, \mathrm{JSF}),$$

where the indices A and L indicate the all-jets and lepton+jets channel, respectively.

No extra calibration of the mass extraction is performed, but the single-channel calibrations are applied. Figure 4 shows the extracted values for the top quark mass and JSF for different input values as a validation. No residual dependence is observed.

The systematic uncertainties are evaluated as described above for the all-jets channel. For the pseudo-experiments, the systematic uncertainty sources are varied simultaneously for both channels. An exception are uncertainties that only affect a single channel. These uncertainty sources are only varied for the corresponding channel. For the all-jets channel, these are the background and trigger uncertainties. In addition, uncertainties specific to the lepton+jets channel are introduced, including the background and trigger uncertainties, as well as the uncertainties arising from the lepton isolation and identification criteria, and are described in Ref.

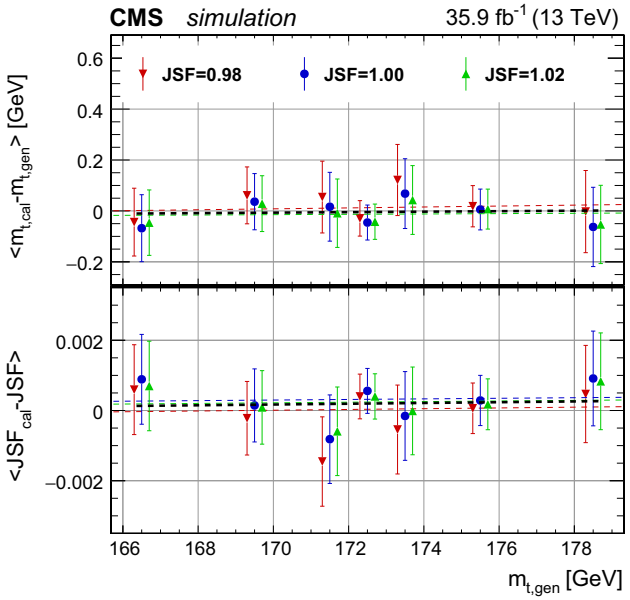

Fig. 4 Difference between extracted and generated top quark masses (upper panel) and JSFs (lower panel) for different input masses and JSFs after the single-channel calibrations for the combined measurement. The values are extracted using the 2D method

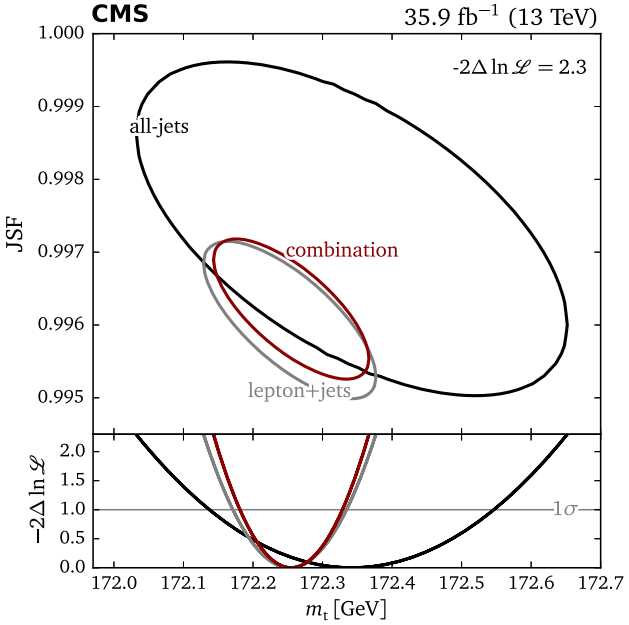

Fig. 5 Likelihood contours for $-2\Delta \ln \mathcal{L} = 2.3$, corresponding to the 68% confidence level, in the m_t-JSF plane (upper panel) and the likelihood profiles for the top quark mass (lower panel), where the level corresponding to one standard deviation (σ) is indicated. The hybrid measurement results for the all-jets and lepton+jets channels, as well as for the combination, are shown

[17]. The complete list of uncertainties is shown in Table 2. A comparison of the hybrid mass uncertainties can be found in Table 3 for the all-jets and lepton+jets channels as well as for the combination. In general, the uncertainties for the combination are smaller than those for the all-jets channel and are close to the lepton+jets uncertainties, as expected because the combination is dominated by this channel. The total uncertainty for the combination is slightly smaller than that for the lepton+jets channel.

The combined measurement yields

$$m_t^{2D} = 172.39 \pm 0.08\,(\text{stat+JSF}) \pm 0.71\,(\text{syst})\,\text{GeV and}$$
$$\text{JSF}^{2D} = 0.995 \pm 0.001\,(\text{stat}) \pm 0.010\,(\text{syst})$$

for the 2D method and

$$m_t^{1D} = 171.94 \pm 0.05\,(\text{stat}) \pm 1.07\,(\text{syst})\,\text{GeV},$$
$$m_t^{\text{hyb}} = 172.26 \pm 0.07\,(\text{stat+JSF}) \pm 0.61\,(\text{syst})\,\text{GeV, and}$$
$$\text{JSF}^{\text{hyb}} = 0.996 \pm 0.001\,(\text{stat}) \pm 0.007\,(\text{syst})$$

for the 1D and hybrid fits. The likelihood contours for $-2\Delta \ln \mathcal{L} = 2.3$, corresponding to the 68% confidence level, in the m_t-JSF plane are shown in Fig. 5 for the hybrid measurement results for the all-jets and lepton+jets channels, as well as for the combination. Additionally, the likelihood profiles are displayed as a function of m_t. Both channels are in statistical agreement with each other. The result of the combination is closer to the lepton+jets channel, as expected.

Just as for the single-channel results, the hybrid measurement provides the best precision and is considered the main result. This is the first top quark mass measurement using the $t\bar{t}$ lepton+jets and all-jets final states combined in a single likelihood function. The largest uncertainty contribution is related to the modeling of color reconnection, as it was observed for the all-jets channel and the lepton+jets channel before using the same CR models. Accordingly, the quoted systematic uncertainty is larger than those reported in the most precise combination reported by the CMS Collaboration [12], and comparable to the value reported by the ATLAS Collaboration [50].

9 Summary

A measurement of the top quark mass (m_t) using the all-jets final state is presented. The analyzed data set was collected by the CMS experiment in proton–proton collisions at $\sqrt{s} = 13$ TeV that correspond to an integrated luminosity of 35.9 fb^{-1}. The kinematic properties in each event are reconstructed using a constrained fit that assumes a $t\bar{t}$ hypothesis, which suppresses the dominant multijet background and improves the mass resolution.

The value of m_t and an additional jet energy scale factor (JSF) are extracted using the ideogram method, which uses the likelihood of the values of m_t and JSF in each event to

Table 2 List of systematic uncertainties for the combined mass extraction. The signs of the shifts ($\delta x = x_{\text{variation}} - x_{\text{nominal}}$) correspond to the +1 standard deviation variation of the systematic uncertainty source. For linear sums of the uncertainty groups, the relative signs have been considered. Shifts determined using dedicated samples for the systematic variation are displayed with the corresponding statistical uncertainty

	2D		1D	Hybrid	
	$\delta m_{\text{t}}^{\text{2D}}$ [GeV]	$\delta\text{JSF}^{\text{2D}}$ [%]	$\delta m_{\text{t}}^{\text{1D}}$ [GeV]	$\delta m_{\text{t}}^{\text{hyb}}$ [GeV]	$\delta\text{JSF}^{\text{hyb}}$ [%]
Experimental uncertainties					
Method calibration	0.03	0.0	0.03	0.03	0.0
JEC (quad. sum)	0.12	0.2	0.82	0.17	0.3
Intercalibration	−0.01	0.0	+0.16	+0.04	+0.1
MPFInSitu	−0.01	0.0	+0.23	+0.07	+0.1
Uncorrelated	−0.12	−0.2	+0.77	+0.15	+0.3
Jet energy resolution	−0.18	+0.3	+0.09	−0.10	+0.2
b tagging	0.03	0.0	0.01	0.02	0.0
Pileup	−0.07	+0.1	+0.02	−0.05	+0.1
All-jets background	0.01	0.0	0.00	0.01	0.0
All-jets trigger	+0.01	0.0	0.00	+0.01	0.0
ℓ+jets Background	−0.02	0.0	+0.01	−0.01	0.0
ℓ+jets Trigger	0.00	0.0	0.00	0.00	0.0
Lepton isolation	0.00	0.0	0.00	0.00	0.0
Lepton identification	0.00	0.0	0.00	0.00	0.0
Modeling uncertainties					
JEC flavor (linear sum)	−0.39	+0.1	−0.31	−0.37	+0.1
Light quarks (uds)	+0.11	−0.1	−0.01	+0.07	−0.1
Charm	+0.03	0.0	−0.01	+0.02	0.0
Bottom	−0.31	0.0	−0.31	−0.31	0.0
Gluon	−0.22	+0.3	+0.02	−0.15	+0.2
b jet modeling (quad. sum)	0.08	0.1	0.04	0.06	0.1
b frag. Bowler–Lund	−0.06	+0.1	−0.01	−0.05	0.0
b frag. Peterson	−0.03	0.0	0.00	−0.02	0.0
semileptonic b hadron decays	−0.04	0.0	−0.04	−0.04	0.0
PDF	0.01	0.0	0.01	0.01	0.0
Ren. and fact. scales	0.01	0.0	0.02	0.01	0.0
ME/PS matching	−0.10 ± 0.08	+0.1	+0.02 ± 0.05	+0.07 ± 0.07	+0.1
ME generator	+0.16 ± 0.21	+0.2	+0.32 ± 0.13	+0.21 ± 0.18	+0.1
ISR PS scale	+0.07 ± 0.08	+0.1	+0.10 ± 0.05	+0.07 ± 0.07	0.1
FSR PS scale	+0.23 ± 0.07	−0.4	−0.19 ± 0.04	+0.12 ± 0.06	−0.3
Top quark p_{T}	+0.01	−0.1	−0.06	−0.01	−0.1
Underlying event	−0.06 ± 0.07	+0.1	+0.00 ± 0.05	−0.04 ± 0.06	+0.1
Early resonance decays	−0.20 ± 0.08	+0.7	+0.42 ± 0.05	−0.01 ± 0.07	+0.5
CR modeling (max. shift)	+0.37 ± 0.09	−0.2	+0.22 ± 0.06	+0.33 ± 0.07	−0.1
"gluon move" (ERD on)	+0.37 ± 0.09	−0.2	+0.22 ± 0.06	+0.33 ± 0.07	−0.1
"QCD inspired" (ERD on)	−0.11 ± 0.09	−0.1	−0.21 ± 0.06	−0.14 ± 0.07	−0.1
Total systematic	0.71	1.0	1.07	0.61	0.7
Statistical (expected)	0.08	0.1	0.05	0.07	0.1
Total (expected)	0.72	1.0	1.08	0.61	0.7

Table 3 Comparison of the hybrid mass uncertainties for the all-jets and lepton+jets [17] channels, as well as the combination. The signs of the shifts follow the convention of Tables 1 and 2

	δm_t^{hyb} [GeV]		
	All-jets	ℓ+jets	Combination
Experimental uncertainties			
Method calibration	0.06	0.05	0.03
JEC (quad. sum)	0.15	0.18	0.17
Intercalibration	−0.04	+0.04	+0.04
MPFInSitu	+0.08	+0.07	+0.07
Uncorrelated	+0.12	+0.16	+0.15
Jet energy resolution	−0.04	−0.12	−0.10
b tagging	0.02	0.03	0.02
Pileup	−0.04	−0.05	−0.05
All-jets background	0.07	–	0.01
All-jets trigger	+0.02	–	+0.01
ℓ+jets background	–	+0.02	−0.01
Modeling uncertainties			
JEC flavor (linear sum)	−0.34	−0.39	−0.37
light quarks (uds)	+0.07	+0.06	+0.07
charm	+0.02	+0.01	+0.02
bottom	−0.29	−0.32	−0.31
gluon	−0.13	−0.15	−0.15
b jet modeling (quad. sum)	0.09	0.12	0.06
b frag. Bowler–Lund	−0.07	−0.05	−0.05
b frag. Peterson	−0.05	+0.04	−0.02
semileptonic b hadron decays	−0.03	+0.10	−0.04
PDF	0.01	0.02	0.01
Ren. and fact. scales	0.04	0.01	0.01
ME/PS matching	+0.24	−0.07	+0.07
ME generator	–	+0.20	+0.21
ISR PS scale	+0.14	+0.07	+0.07
FSR PS scale	+0.18	+0.13	+0.12
Top quark p_T	+0.03	−0.01	−0.01
Underlying event	+0.17	−0.07	−0.06
Early resonance decays	+0.24	−0.07	−0.07
CR modeling (max. shift)	−0.36	+0.31	+0.33
"gluon move" (ERD on)	+0.32	+0.31	+0.33
"QCD inspired" (ERD on)	−0.36	−0.13	−0.14
Total systematic	0.70	0.62	0.61
Statistical (expected)	0.20	0.08	0.07
Total (expected)	0.72	0.63	0.61

determine these parameters. The resulting m_t is measured to be 172.34±0.20 (stat+JSF)±0.70 (syst) GeV. This is in good agreement with previous CMS results obtained at $\sqrt{s} = 7$, 8, and 13 TeV. The modeling uncertainties are larger than in the previous measurements at lower center-of-mass energies because of the use of new alternative color reconnection models that were not previously available.

A combined measurement using also the lepton+jets final state results in $m_t = 172.26 \pm 0.07\,(\text{stat+JSF}) \pm 0.61\,(\text{syst})$ GeV. This is the first combined m_t result obtained in the all-jets and lepton+jets final states using a single likelihood function.

Acknowledgements We congratulate our colleagues in the CERN accelerator departments for the excellent performance of the LHC and thank the technical and administrative staffs at CERN and at other CMS institutes for their contributions to the success of the CMS effort. In addition, we gratefully acknowledge the computing centers and personnel of the Worldwide LHC Computing Grid for delivering so effec-

tively the computing infrastructure essential to our analyses. Finally, we acknowledge the enduring support for the construction and operation of the LHC and the CMS detector provided by the following funding agencies: BMBWF and FWF (Austria); FNRS and FWO (Belgium); CNPq, CAPES, FAPERJ, FAPERGS, and FAPESP (Brazil); MES (Bulgaria); CERN; CAS, MoST, and NSFC (China); COLCIENCIAS (Colombia); MSES and CSF (Croatia); RPF (Cyprus); SENESCYT (Ecuador); MoER, ERC IUT, and ERDF (Estonia); Academy of Finland, MEC, and HIP (Finland); CEA and CNRS/IN2P3 (France); BMBF, DFG, and HGF (Germany); GSRT (Greece); NKFIA (Hungary); DAE and DST (India); IPM (Iran); SFI (Ireland); INFN (Italy); MSIP and NRF (Republic of Korea); MES (Latvia); LAS (Lithuania); MOE and UM (Malaysia); BUAP, CINVESTAV, CONACYT, LNS, SEP, and UASLP-FAI (Mexico); MOS (Montenegro); MBIE (New Zealand); PAEC (Pakistan); MSHE and NSC (Poland); FCT (Portugal); JINR (Dubna); MON, RosAtom, RAS, RFBR, and NRC KI (Russia); MESTD (Serbia); SEIDI, CPAN, PCTI, and FEDER (Spain); MOSTR (Sri Lanka); Swiss Funding Agencies (Switzerland); MST (Taipei); ThEPCenter, IPST, STAR, and NSTDA (Thailand); TUBITAK and TAEK (Turkey); NASU and SFFR (Ukraine); STFC (UK); DOE and NSF (USA). Individuals have received support from the Marie-Curie program and the European Research Council and Horizon 2020 Grant, contract No. 675440 (European Union); the Leventis Foundation; the A.P. Sloan Foundation; the Alexander von Humboldt Foundation; the Belgian Federal Science Policy Office; the Fonds pour la Formation à la Recherche dans l'Industrie et dans l'Agriculture (FRIA-Belgium); the Agentschap voor Innovatie door Wetenschap en Technologie (IWT-Belgium); the F.R.S.-FNRS and FWO (Belgium) under the "Excellence of Science – EOS" – be.h project n. 30820817; the Ministry of Education, Youth and Sports (MEYS) of the Czech Republic; the Lendület ("Momentum") Programme and the János Bolyai Research Scholarship of the Hungarian Academy of Sciences, the New National Excellence Program ÚNKP, the NKFIA research Grants 123842, 123959, 124845, 124850, and 125105 (Hungary); the Council of Science and Industrial Research, India; the HOMING PLUS program of the Foundation for Polish Science, cofinanced from European Union, Regional Development Fund, the Mobility Plus program of the Ministry of Science and Higher Education, the National Science Center (Poland), contracts Harmonia 2014/14/M/ST2/00428, Opus 2014/13/B/ST2/02543, 2014/15/B/ST2/03998, and 2015/19/B/ST2/02861, Sonata-bis 2012/07/E/ST2/01406; the National Priorities Research Program by Qatar National Research Fund; the Programa Estatal de Fomento de la Investigación Científica y Técnica de Excelencia María de Maeztu, Grant MDM-2015-0509 and the Programa Severo Ochoa del Principado de Asturias; the Thalis and Aristeia programs cofinanced by EU-ESF and the Greek NSRF; the Rachadapisek Sompot Fund for Postdoctoral Fellowship, Chulalongkorn University and the Chulalongkorn Academic into Its 2nd Century Project Advancement Project (Thailand); the Welch Foundation, contract C-1845; and the Weston Havens Foundation (USA).

Data Availability Statement This manuscript has no associated data or the data will not be deposited. [Authors' comment: Release and preservation of data used by the CMS Collaboration as the basis for publications is guided by the CMS policy as written in its document "CMS data preservation, re-use and open access policy" (https://cms-docdb.cern.ch/cgi-bin/PublicDocDB/RetrieveFile?docid=6032&filename=CMSDataPolicyV1.2.pdf&version=2).]

Funded by SCOAP[3].

References

1. CDF Collaboration, Observation of top quark production in $\bar{p}p$ collisions. Phys. Rev. Lett. **74**, 2626 (1995). https://doi.org/10.1103/PhysRevLett.74.2626. arXiv:hep-ex/9503002
2. D0 Collaboration, Observation of the top quark. Phys. Rev. Lett. **74**, 2632 (1995). https://doi.org/10.1103/PhysRevLett.74.2632. arXiv:hep-ex/9503003
3. The ALEPH, CDF, D0, DELPHI, L3, OPAL, SLD Collaborations, the LEP Electroweak Working Group, the Tevatron Electroweak Working Group, and the SLD electroweak and heavy flavour groups, "Precision Electroweak Measurements and Constraints on the Standard Model", technical report, 2010. arXiv:1012.2367
4. M. Baak et al., The electroweak fit of the standard model after the discovery of a new boson at the LHC. Eur. Phys. J. C **72**, 2205 (2012). https://doi.org/10.1140/epjc/s10052-012-2205-9. arXiv:1209.2716
5. M. Baak et al., The global electroweak fit at NNLO and prospects for the LHC and ILC. Eur. Phys. J. C **74**, 3046 (2014). https://doi.org/10.1140/epjc/s10052-014-3046-5. arXiv:1407.3792
6. G. Degrassi et al., Higgs mass and vacuum stability in the standard model at NNLO. JHEP **08**, 1 (2012). https://doi.org/10.1007/JHEP08(2012)098. arXiv:1205.6497
7. F. Bezrukov, M.Y. Kalmykov, B.A. Kniehl, M. Shaposhnikov, Higgs boson mass and new physics. JHEP **10**, 140 (2012). https://doi.org/10.1007/JHEP10(2012)140. arXiv:1205.2893
8. DELPHI Collaboration, Measurement of the mass and width of the W boson in e^+e^- collisions at $\sqrt{s} = 161 - 209$ GeV, *Eur. Phys. J. C* **55**, 1 (2008). https://doi.org/10.1140/epjc/s10052-008-0585-7. arXiv:0803.2534
9. CMS Collaboration, Measurement of the top-quark mass in $t\bar{t}$ events with lepton+jets final states in pp collisions at $\sqrt{s} = 7$ TeV. JHEP **12**, 105 (2012). https://doi.org/10.1007/JHEP12(2012)105. arXiv:1209.2319
10. CDF Collaboration, Measurement of the top-quark mass in the all-hadronic channel using the full CDF data set. Phys. Rev. D **90**, 091101 (2014). https://doi.org/10.1103/PhysRevD.90.091101. arXiv:1409.4906
11. CMS Collaboration, Measurement of the top-quark mass in all-jets $t\bar{t}$ events in pp collisions at $\sqrt{s}$=7 TeV. Eur. Phys. J. C **74**, 2758 (2014). https://doi.org/10.1140/epjc/s10052-014-2758-x. arXiv:1307.4617
12. CMS Collaboration, Measurement of the top quark mass using proton-proton data at $\sqrt{s}$ = 7 and 8 TeV. Phys. Rev. D **93**, 072004 (2016). https://doi.org/10.1103/PhysRevD.93.072004. arXiv:1509.04044
13. ATLAS Collaboration, Measurement of the top-quark mass in the fully hadronic decay channel from ATLAS data at $\sqrt{s} = 7$ TeV, *Eur. Phys. J. C* **75**, 158 (2015). https://doi.org/10.1140/epjc/s10052-015-3373-1. arXiv:1409.0832
14. ATLAS Collaboration, Top-quark mass measurement in the all-hadronic $t\bar{t}$ decay channel at $\sqrt{s} = 8$ TeV with the ATLAS detector, *JHEP* **09**, 118 (2017). https://doi.org/10.1007/JHEP09(2017)118. arXiv:1702.07546
15. ATLAS Collaboration, Measurement of the top quark mass in the $t\bar{t} \to$ lepton+jets channel from $\sqrt{s} = 8$ TeV ATLAS data and combination with previous results, (2018). arXiv:1810.01772. Submitted to Eur. Phys. J. C
16. CDF and D0 Collaborations, Combination of CDF and D0 results on the mass of the top quark using up 9.7 fb^{-1} at the Tevatron, FERMILAB-CONF-16-298-E, TEVEWWG/top2016/01. arXiv:1608.01881 (2016)

17. CMS Collaboration, Measurement of the top quark mass with lepton+jets final states using pp collisions at $\sqrt{s} = 13$ TeV. Eur. Phys. J. C. **78**, 891 (2018). https://doi.org/10.1140/epjc/s10052-018-6332-9. arXiv:1805.01428
18. CMS Collaboration, The CMS trigger system. JINST **12**, P01020 (2017). https://doi.org/10.1088/1748-0221/12/01/P01020. arXiv:1609.02366
19. CMS Collaboration, Particle-flow reconstruction and global event description with the CMS detector. JINST **12**, P10003 (2017). https://doi.org/10.1088/1748-0221/12/10/P10003. arXiv:1706.04965
20. M. Cacciari, G.P. Salam, G. Soyez, The anti-k_T jet clustering algorithm. JHEP **04**, 063 (2008). https://doi.org/10.1088/1126-6708/2008/04/063. arXiv:0802.1189
21. M. Cacciari, G.P. Salam, G. Soyez, FastJet user manual. Eur. Phys. J. C **72**, 1896 (2012). https://doi.org/10.1140/epjc/s10052-012-1896-2. arXiv:1111.6097
22. M. Cacciari, G.P. Salam, Dispelling the N^3 myth for the k_t jet-finder. Phys. Lett. B **641**, 57 (2006). https://doi.org/10.1016/j.physletb.2006.08.037. arXiv:hep-ph/0512210
23. CMS Collaboration, Jet energy scale and resolution in the CMS experiment in pp collisions at 8 TeV. JINST **12**, P02014 (2017). https://doi.org/10.1088/1748-0221/12/02/P02014. arXiv:1607.03663
24. CMS Collaboration, Jet algorithms performance in 13 TeV data, CMS Physics Analysis Summary CMS-PAS-JME-16-003 (2017). http://cds.cern.ch/record/2256875
25. CMS Collaboration, The CMS experiment at the CERN LHC. JINST **3**, S08004 (2008). https://doi.org/10.1088/1748-0221/3/08/S08004
26. CMS Collaboration, Identification of heavy-flavour jets with the CMS detector in pp collisions at 13 TeV. JINST **13**, P05011 (2018). https://doi.org/10.1088/1748-0221/13/05/P05011. arXiv:1712.07158
27. P. Nason, A new method for combining NLO QCD with shower Monte Carlo algorithms. JHEP **11**, 040 (2004). https://doi.org/10.1088/1126-6708/2004/11/040. arXiv:hep-ph/0409146
28. S. Frixione, P. Nason, C. Oleari, Matching NLO QCD computations with parton shower simulations: the powheg method. JHEP **11**, 070 (2007). https://doi.org/10.1088/1126-6708/2007/11/070. arXiv:0709.2092
29. S. Alioli, P. Nason, C. Oleari, E. Re, A general framework for implementing NLO calculations in shower Monte Carlo programs: the powheg BOX. JHEP **06**, 043 (2010). https://doi.org/10.1007/JHEP06(2010)043. arXiv:1002.2581
30. NNPDF Collaboration, Parton distributions for the LHC Run II", *JHEP* **04**, 040 (2015). https://doi.org/10.1007/JHEP04(2015)040. arXiv:1410.8849
31. T. Sjöstrand, S. Mrenna, and P. Z. Skands, A brief introduction to PYTHIA 8.1, *Comput. Phys. Commun.* **178**, 852 (2008). https://doi.org/10.1016/j.cpc.2008.01.036. arXiv:0710.3820
32. P. Skands, S. Carrazza, J. Rojo, Tuning PYTHIA 8.1: the Monash 2013 Tune. Eur. Phys. J. C **74**(2014), 3024 (2013). https://doi.org/10.1140/epjc/s10052-014-3024-y. arXiv:1404.5630
33. CMS Collaboration, Investigations of the impact of the parton shower tuning in PYTHIA 8 in the modelling of $t\bar{t}$ at $\sqrt{s} = 8$ and 13 TeV. CMS Physics Analysis Summary CMS-PAS-TOP-16-021 (2016). https://cds.cern.ch/record/2235192
34. GEANT4 Collaboration, GEANT4—a simulation toolkit. Nucl. Instrum. Meth. A **506**, 250 (2003). https://doi.org/10.1016/S0168-9002(03)01368-8
35. M. Czakon, A. Mitov, Top++: A program for the calculation of the top-pair cross-section at hadron colliders. Comput. Phys. Commun. **185**, 2930 (2014). https://doi.org/10.1016/j.cpc.2014.06.021. arXiv:1112.5675
36. ATLAS and CMS Collaborations, "Jet energy scale uncertainty correlations between ATLAS and CMS at 8 TeV", ATL-PHYS-PUB-2015-049, CMS-PAS-JME-15-001 (2015). http://cds.cern.ch/record/2104039
37. CMS Collaboration, Measurement of the inelastic proton-proton cross section at $\sqrt{s} = 13$ TeV. JHEP **07**, 161 (2018). https://doi.org/10.1007/JHEP07(2018)161. arXiv:1802.02613
38. T. Sjöstrand, S. Mrenna, P. Skands, PYTHIA 6.4 physics and manual. JHEP **05**, 026 (2006). https://doi.org/10.1088/1126-6708/2006/05/026. arXiv:hep-ph/0603175
39. M. Bähr et al., Herwig++ physics and manual. Eur. Phys. J. C **58**, 639 (2008). https://doi.org/10.1140/epjc/s10052-008-0798-9. arXiv:0803.0883
40. DELPHI Collaboration, A study of the b-quark fragmentation function with the DELPHI detector at LEP I and an averaged distribution obtained at the Z Pole. Eur. Phys. J. C **71**, 1557 (2011). https://doi.org/10.1140/epjc/s10052-011-1557-x. arXiv:1102.4748
41. ALEPH Collaboration, Study of the fragmentation of b quarks into B mesons at the Z peak. Phys. Lett. B **512**, 30 (2001). https://doi.org/10.1016/S0370-2693(01)00690-6. arXiv:hep-ex/0106051
42. Particle Data Group, Review of particle physics. Chin. Phys. C **40**, 100001 (2016). https://doi.org/10.1088/1674-1137/40/10/100001
43. M. Czakon, D. Heymes, A. Mitov, High-precision differential predictions for top-quark pairs at the LHC. Phys. Rev. Lett. **116**, 082003 (2016). https://doi.org/10.1103/PhysRevLett.116.082003. arXiv:1511.00549
44. CMS Collaboration, Measurement of differential cross sections for top quark pair production using the lepton+jets final state in proton-proton collisions at 13 TeV. Phys. Rev. D **95**, 092001 (2017). https://doi.org/10.1103/PhysRevD.95.092001. arXiv:1610.04191
45. CMS Collaboration, Measurement of normalized differential $t\bar{t}$ cross sections in the dilepton channel from pp collisions at $\sqrt{s} = 13$ TeV. JHEP **04**, 060 (2018). https://doi.org/10.1007/JHEP04(2018)060. arXiv:1708.07638
46. J.R. Christiansen, P.Z. Skands, String formation beyond leading colour. JHEP **08**, 003 (2015). https://doi.org/10.1007/JHEP08(2015)003. arXiv:1505.01681
47. S. Argyropoulos, T. Sjöstrand, Effects of color reconnection on $t\bar{t}$ final states at the LHC. JHEP **11**, 043 (2014). https://doi.org/10.1007/JHEP11(2014)043. arXiv:1407.6653
48. J. Alwall et al., The automated computation of tree-level and next-to-leading order differential cross sections, and their matching to parton shower simulations. JHEP **07**, 079 (2014). https://doi.org/10.1007/JHEP07(2014)079. arXiv:1405.0301
49. R. Frederix, S. Frixione, Merging meets matching in MC@NLO. JHEP **12**, 061 (2012). https://doi.org/10.1007/JHEP12(2012)061. arXiv:1209.6215
50. ATLAS Collaboration, Measurement of the top quark mass in the $t\bar{t} \rightarrow$ dilepton channel from $\sqrt{s} = 8$ TeV ATLAS data. Phys. Lett. B **761**, 350 (2016). https://doi.org/10.1016/j.physletb.2016.08.042. arXiv:1606.02179

CMS Collaboration

Yerevan Physics Institute, Yerevan, Armenia
A. M. Sirunyan, A. Tumasyan

Institut für Hochenergiephysik, Wien, Austria
W. Adam, F. Ambrogi, E. Asilar, T. Bergauer, J. Brandstetter, M. Dragicevic, J. Erö, A. Escalante Del Valle, M. Flechl, R. Frühwirth[1], V. M. Ghete, J. Hrubec, M. Jeitler[1], N. Krammer, I. Krätschmer, D. Liko, T. Madlener, I. Mikulec, N. Rad, H. Rohringer, J. Schieck[1], R. Schöfbeck, M. Spanring, D. Spitzbart, W. Waltenberger, J. Wittmann, C.-E. Wulz[1], M. Zarucki

Institute for Nuclear Problems, Minsk, Belarus
V. Chekhovsky, V. Mossolov, J. Suarez Gonzalez

Universiteit Antwerpen, Antwerpen, Belgium
E. A. De Wolf, D. Di Croce, X. Janssen, J. Lauwers, A. Lelek, M. Pieters, H. Van Haevermaet, P. Van Mechelen, N. Van Remortel

Vrije Universiteit Brussel, Brussel, Belgium
S. Abu Zeid, F. Blekman, J. D'Hondt, J. De Clercq, K. Deroover, G. Flouris, D. Lontkovskyi, S. Lowette, I. Marchesini, S. Moortgat, L. Moreels, Q. Python, K. Skovpen, S. Tavernier, W. Van Doninck, P. Van Mulders, I. Van Parijs

Université Libre de Bruxelles, Bruxelles, Belgium
D. Beghin, B. Bilin, H. Brun, B. Clerbaux, G. De Lentdecker, H. Delannoy, B. Dorney, G. Fasanella, L. Favart, A. Grebenyuk, A. K. Kalsi, T. Lenzi, J. Luetic, N. Postiau, E. Starling, L. Thomas, C. Vander Velde, P. Vanlaer, D. Vannerom, Q. Wang

Ghent University, Ghent, Belgium
T. Cornelis, D. Dobur, A. Fagot, M. Gul, I. Khvastunov[2], D. Poyraz, C. Roskas, D. Trocino, M. Tytgat, W. Verbeke, B. Vermassen, M. Vit, N. Zaganidis

Université Catholique de Louvain, Louvain-la-Neuve, Belgium
H. Bakhshiansohi, O. Bondu, G. Bruno, C. Caputo, P. David, C. Delaere, M. Delcourt, A. Giammanco, G. Krintiras, V. Lemaitre, A. Magitteri, K. Piotrzkowski, A. Saggio, M. Vidal Marono, P. Vischia, J. Zobec

Centro Brasileiro de Pesquisas Fisicas, Rio de Janeiro, Brazil
F. L. Alves, G. A. Alves, G. Correia Silva, C. Hensel, A. Moraes, M. E. Pol, P. Rebello Teles

Universidade do Estado do Rio de Janeiro, Rio de Janeiro, Brazil
E. Belchior Batista Das Chagas, W. Carvalho, J. Chinellato[3], E. Coelho, E. M. Da Costa, G. G. Da Silveira[4], D. De Jesus Damiao, C. De Oliveira Martins, S. Fonseca De Souza, H. Malbouisson, D. Matos Figueiredo, M. Melo De Almeida, C. Mora Herrera, L. Mundim, H. Nogima, W. L. Prado Da Silva, L. J. Sanchez Rosas, A. Santoro, A. Sznajder, M. Thiel, E. J. Tonelli Manganote[3], F. Torres Da Silva De Araujo, A. Vilela Pereira

Universidade Estadual Paulista[a], Universidade Federal do ABC[b], São Paulo, Brazil
S. Ahuja[a], C. A. Bernardes[a], L. Calligaris[a], T. R. Fernandez Perez Tomei[a], E. M. Gregores[b], P. G. Mercadante[b], S. F. Novaes[a], SandraS. Padula[a]

Institute for Nuclear Research and Nuclear Energy, Bulgarian Academy of Sciences, Sofia, Bulgaria
A. Aleksandrov, R. Hadjiiska, P. Iaydjiev, A. Marinov, M. Misheva, M. Rodozov, M. Shopova, G. Sultanov

University of Sofia, Sofia, Bulgaria
A. Dimitrov, L. Litov, B. Pavlov, P. Petkov

Beihang University, Beijing, China
W. Fang[5], X. Gao[5], L. Yuan

Institute of High Energy Physics, Beijing, China
M. Ahmad, J. G. Bian, G. M. Chen, H. S. Chen, M. Chen, Y. Chen, C. H. Jiang, D. Leggat, H. Liao, Z. Liu, S. M. Shaheen[6], A. Spiezia, J. Tao, E. Yazgan, H. Zhang, S. Zhang[6], J. Zhao

State Key Laboratory of Nuclear Physics and Technology, Peking University, Beijing, China
Y. Ban, G. Chen, A. Levin, J. Li, L. Li, Q. Li, Y. Mao, S. J. Qian, D. Wang

Tsinghua University, Beijing, China
Y. Wang

Universidad de Los Andes, Bogota, Colombia
C. Avila, A. Cabrera, C. A. Carrillo Montoya, L. F. Chaparro Sierra, C. Florez, C. F. González Hernández, M. A. Segura Delgado

Faculty of Electrical Engineering, Mechanical Engineering and Naval Architecture, University of Split, Split, Croatia
B. Courbon, N. Godinovic, D. Lelas, I. Puljak, T. Sculac

Faculty of Science, University of Split, Split, Croatia
Z. Antunovic, M. Kovac

Institute Rudjer Boskovic, Zagreb, Croatia
V. Brigljevic, D. Ferencek, K. Kadija, B. Mesic, M. Roguljic, A. Starodumov[7], T. Susa

University of Cyprus, Nicosia, Cyprus
M. W. Ather, A. Attikis, M. Kolosova, G. Mavromanolakis, J. Mousa, C. Nicolaou, F. Ptochos, P. A. Razis, H. Rykaczewski

Charles University, Prague, Czech Republic
M. Finger[8], M. Finger Jr.[8]

Escuela Politecnica Nacional, Quito, Ecuador
E. Ayala

Universidad San Francisco de Quito, Quito, Ecuador
E. Carrera Jarrin

Academy of Scientific Research and Technology of the Arab Republic of Egypt, Egyptian Network of High Energy Physics, Cairo, Egypt
H. Abdalla[9], S. Khalil[10], A. Mohamed[10]

National Institute of Chemical Physics and Biophysics, Tallinn, Estonia
S. Bhowmik, A. Carvalho Antunes De Oliveira, R. K. Dewanjee, K. Ehataht, M. Kadastik, M. Raidal, C. Veelken

Department of Physics, University of Helsinki, Helsinki, Finland
P. Eerola, H. Kirschenmann, J. Pekkanen, M. Voutilainen

Helsinki Institute of Physics, Helsinki, Finland
J. Havukainen, J. K. Heikkilä, T. Järvinen, V. Karimäki, R. Kinnunen, T. Lampén, K. Lassila-Perini, S. Laurila, S. Lehti, T. Lindén, P. Luukka, T. Mäenpää, H. Siikonen, E. Tuominen, J. Tuominiemi

Lappeenranta University of Technology, Lappeenranta, Finland
T. Tuuva

IRFU, CEA, Université Paris-Saclay, Gif-sur-Yvette, France
M. Besancon, F. Couderc, M. Dejardin, D. Denegri, J. L. Faure, F. Ferri, S. Ganjour, A. Givernaud, P. Gras, G. Hamel de Monchenault, P. Jarry, C. Leloup, E. Locci, J. Malcles, G. Negro, J. Rander, A. Rosowsky, M. Ö. Sahin, M. Titov

Laboratoire Leprince-Ringuet, Ecole polytechnique, CNRS/IN2P3, Université Paris-Saclay, Palaiseau, France
A. Abdulsalam[11], C. Amendola, I. Antropov, F. Beaudette, P. Busson, C. Charlot, R. Granier de Cassagnac, I. Kucher, A. Lobanov, J. Martin Blanco, C. Martin Perez, M. Nguyen, C. Ochando, G. Ortona, P. Paganini, J. Rembser, R. Salerno, J. B. Sauvan, Y. Sirois, A. G. Stahl Leiton, A. Zabi, A. Zghiche

Université de Strasbourg, CNRS, IPHC UMR 7178, Strasbourg, France
J.-L. Agram[12], J. Andrea, D. Bloch, G. Bourgatte, J.-M. Brom, E. C. Chabert, V Cherepanov, C. Collard, E. Conte[12], J.-C. Fontaine[12], D. Gelé, U. Goerlach, M. Jansová, A.-C. Le Bihan, N. Tonon, P. Van Hove

Centre de Calcul de l'Institut National de Physique Nucleaire et de Physique des Particules, CNRS/IN2P3, Villeurbanne, France
S. Gadrat

Université de Lyon, Université Claude Bernard Lyon 1, CNRS-IN2P3, Institut de Physique Nucléaire de Lyon, Villeurbanne, France
S. Beauceron, C. Bernet, G. Boudoul, N. Chanon, R. Chierici, D. Contardo, P. Depasse, H. El Mamouni, J. Fay, L. Finco, S. Gascon, M. Gouzevitch, G. Grenier, B. Ille, F. Lagarde, I. B. Laktineh, H. Lattaud, M. Lethuillier, L. Mirabito, S. Perries, A. Popov[13], V. Sordini, G. Touquet, M. Vander Donckt, S. Viret

Georgian Technical University, Tbilisi, Georgia
A. Khvedelidze[8]

Tbilisi State University, Tbilisi, Georgia
Z. Tsamalaidze[8]

RWTH Aachen University, I. Physikalisches Institut, Aachen, Germany
C. Autermann, L. Feld, M. K. Kiesel, K. Klein, M. Lipinski, M. Preuten, M. P. Rauch, C. Schomakers, J. Schulz, M. Teroerde, B. Wittmer

RWTH Aachen University, III. Physikalisches Institut A, Aachen, Germany
A. Albert, M. Erdmann, S. Erdweg, T. Esch, R. Fischer, S. Ghosh, A. Güth, T. Hebbeker, C. Heidemann, K. Hoepfner, H. Keller, L. Mastrolorenzo, M. Merschmeyer, A. Meyer, P. Millet, S. Mukherjee, T. Pook, M. Radziej, H. Reithler, M. Rieger, A. Schmidt, D. Teyssier, S. Thüer

RWTH Aachen University, III. Physikalisches Institut B, Aachen, Germany
G. Flügge, O. Hlushchenko, T. Kress, T. Müller, A. Nehrkorn, A. Nowack, C. Pistone, O. Pooth, D. Roy, H. Sert, A. Stahl[14]

Deutsches Elektronen-Synchrotron, Hamburg, Germany
M. Aldaya Martin, T. Arndt, C. Asawatangtrakuldee, I. Babounikau, K. Beernaert, O. Behnke, U. Behrens, A. Bermúdez Martínez, D. Bertsche, A. A. Bin Anuar, K. Borras[15], V. Botta, A. Campbell, P. Connor, C. Contreras-Campana, V. Danilov, A. De Wit, M. M. Defranchis, C. Diez Pardos, D. Domínguez Damiani, G. Eckerlin, T. Eichhorn, A. Elwood, E. Eren, E. Gallo[16], A. Geiser, J. M. Grados Luyando, A. Grohsjean, M. Guthoff, M. Haranko, A. Harb, H. Jung, M. Kasemann, J. Keaveney, C. Kleinwort, J. Knolle, D. Krücker, W. Lange, T. Lenz, J. Leonard, K. Lipka, W. Lohmann[17], R. Mankel, I.-A. Melzer-Pellmann, A. B. Meyer, M. Meyer, M. Missiroli, G. Mittag, J. Mnich, V. Myronenko, S. K. Pflitsch, D. Pitzl, A. Raspereza, A. Saibel, M. Savitskyi, P. Saxena, P. Schütze, C. Schwanenberger, R. Shevchenko, A. Singh, H. Tholen, O. Turkot, A. Vagnerini, M. Van De Klundert, G. P. Van Onsem, R. Walsh, Y. Wen, K. Wichmann, C. Wissing, O. Zenaiev

University of Hamburg, Hamburg, Germany
R. Aggleton, S. Bein, L. Benato, A. Benecke, T. Dreyer, A. Ebrahimi, E. Garutti, D. Gonzalez, P. Gunnellini, J. Haller, A. Hinzmann, A. Karavdina, G. Kasieczka, R. Klanner, R. Kogler, N. Kovalchuk, S. Kurz, V. Kutzner, J. Lange, D. Marconi, J. Multhaup, M. Niedziela, C.E.N. Niemeyer, D. Nowatschin, A. Perieanu, A. Reimers, O. Rieger, C. Scharf, P. Schleper, S. Schumann, J. Schwandt, J. Sonneveld, H. Stadie, G. Steinbrück, F. M. Stober, M. Stöver, B. Vormwald, I. Zoi

Karlsruher Institut fuer Technologie, Karlsruhe, Germany
M. Akbiyik, C. Barth, M. Baselga, S. Baur, E. Butz, R. Caspart, T. Chwalek, F. Colombo, W. De Boer, A. Dierlamm, K. El Morabit, N. Faltermann, B. Freund, M. Giffels, M. A. Harrendorf, F. Hartmann[14], S. M. Heindl, U. Husemann, I. Katkov[13], S. Kudella, S. Mitra, M. U. Mozer, Th. Müller, M. Musich, M. Plagge, G. Quast, K. Rabbertz, M. Schröder, I. Shvetsov, H. J. Simonis, R. Ulrich, S. Wayand, M. Weber, T. Weiler, C. Wöhrmann, R. Wolf

Institute of Nuclear and Particle Physics (INPP), NCSR Demokritos, Aghia Paraskevi, Greece
G. Anagnostou, G. Daskalakis, T. Geralis, A. Kyriakis, D. Loukas, G. Paspalaki

National and Kapodistrian University of Athens, Athens, Greece
A. Agapitos, G. Karathanasis, P. Kontaxakis, A. Panagiotou, I. Papavergou, N. Saoulidou, K. Vellidis

National Technical University of Athens, Athens, Greece
K. Kousouris, I. Papakrivopoulos, G. Tsipolitis

University of Ioánnina, Ioánnina, Greece
I. Evangelou, C. Foudas, P. Gianneios, P. Katsoulis, P. Kokkas, S. Mallios, N. Manthos, I. Papadopoulos, E. Paradas, J. Strologas, F. A. Triantis, D. Tsitsonis

MTA-ELTE Lendület CMS Particle and Nuclear Physics Group, Eötvös Loránd University, Budapest, Hungary
M. Bartók[18], M. Csanad, N. Filipovic, P. Major, M. I. Nagy, G. Pasztor, O. Surányi, G. I. Veres

Wigner Research Centre for Physics, Budapest, Hungary
G. Bencze, C. Hajdu, D. Horvath[19], Á. Hunyadi, F. Sikler, T. Á. Vámi, V. Veszpremi, G. Vesztergombi[†]

Institute of Nuclear Research ATOMKI, Debrecen, Hungary
N. Beni, S. Czellar, J. Karancsi[18], A. Makovec, J. Molnar, Z. Szillasi

Institute of Physics, University of Debrecen, Debrecen, Hungary
P. Raics, Z. L. Trocsanyi, B. Ujvari

Indian Institute of Science (IISc), Bangalore, India
S. Choudhury, J. R. Komaragiri, P. C. Tiwari

National Institute of Science Education and Research, HBNI, Bhubaneswar, India
S. Bahinipati[21], C. Kar, P. Mal, K. Mandal, A. Nayak[22], S. Roy Chowdhury, D. K. Sahoo[21], S. K. Swain

Panjab University, Chandigarh, India
S. Bansal, S. B. Beri, V. Bhatnagar, S. Chauhan, R. Chawla, N. Dhingra, R. Gupta, A. Kaur, M. Kaur, S. Kaur, P. Kumari, M. Lohan, M. Meena, A. Mehta, K. Sandeep, S. Sharma, J. B. Singh, A. K. Virdi, G. Walia

University of Delhi, Delhi, India
A. Bhardwaj, B. C. Choudhary, R. B. Garg, M. Gola, S. Keshri, Ashok Kumar, S. Malhotra, M. Naimuddin, P. Priyanka, K. Ranjan, Aashaq Shah, R. Sharma

Saha Institute of Nuclear Physics, HBNI, Kolkata, India
R. Bhardwaj[23], M. Bharti[23], R. Bhattacharya, S. Bhattacharya, U. Bhawandeep[23], D. Bhowmik, S. Dey, S. Dutt[23], S. Dutta, S. Ghosh, M. Maity[24], K. Mondal, S. Nandan, A. Purohit, P. K. Rout, A. Roy, G. Saha, S. Sarkar, T. Sarkar[24], M. Sharan, B. Singh[23], S. Thakur[23]

Indian Institute of Technology Madras, Madras, India
P. K. Behera, A. Muhammad

Bhabha Atomic Research Centre, Mumbai, India
R. Chudasama, D. Dutta, V. Jha, V. Kumar, D. K. Mishra, P. K. Netrakanti, L. M. Pant, P. Shukla, P. Suggisetti

Tata Institute of Fundamental Research-A, Mumbai, India
T. Aziz, M. A. Bhat, S. Dugad, G. B. Mohanty, N. Sur, RavindraKumar Verma

Tata Institute of Fundamental Research-B, Mumbai, India
S. Banerjee, S. Bhattacharya, S. Chatterjee, P. Das, M. Guchait, Sa. Jain, S. Karmakar, S. Kumar, G. Majumder, K. Mazumdar, N. Sahoo

Indian Institute of Science Education and Research (IISER), Pune, India
S. Chauhan, S. Dube, V. Hegde, A. Kapoor, K. Kothekar, S. Pandey, A. Rane, A. Rastogi, S. Sharma

Institute for Research in Fundamental Sciences (IPM), Tehran, Iran
S. Chenarani[25], E. Eskandari Tadavani, S. M. Etesami[25], M. Khakzad, M. Mohammadi Najafabadi, M. Naseri, F. Rezaei Hosseinabadi, B. Safarzadeh[26], M. Zeinali

University College Dublin, Dublin, Ireland
M. Felcini, M. Grunewald

INFN Sezione di Bari[a], Università di Bari[b], Politecnico di Bari[c], Bari, Italy
M. Abbrescia[a,b], C. Calabria[a,b], A. Colaleo[a], D. Creanza[a,c], L. Cristella[a,b], N. De Filippis[a,c], M. De Palma[a,b], A. Di Florio[a,b], F. Errico[a,b], L. Fiore[a], A. Gelmi[a,b], G. Iaselli[a,c], M. Ince[a,b], S. Lezki[a,b], G. Maggi[a,c], M. Maggi[a], G. Miniello[a,b], S. My[a,b], S. Nuzzo[a,b], A. Pompili[a,b], G. Pugliese[a,c], R. Radogna[a], A. Ranieri[a], G. Selvaggi[a,b], A. Sharma[a], L. Silvestris[a], R. Venditti[a], P. Verwilligen[a]

INFN Sezione di Bologna[a], Università di Bologna[b], Bologna, Italy
G. Abbiendi[a], C. Battilana[a,b], D. Bonacorsi[a,b], L. Borgonovi[a,b], S. Braibant-Giacomelli[a,b], R. Campanini[a,b], P. Capiluppi[a,b], A. Castro[a,b], F. R. Cavallo[a], S. S. Chhibra[a,b], G. Codispoti[a,b], M. Cuffiani[a,b], G. M. Dallavalle[a], F. Fabbri[a], A. Fanfani[a,b], E. Fontanesi, P. Giacomelli[a], C. Grandi[a], L. Guiducci[a,b], F. Iemmi[a,b], S. Lo Meo[a,27], S. Marcellini[a], G. Masetti[a], A. Montanari[a], F. L. Navarria[a,b], A. Perrotta[a], F. Primavera[a,b], A. M. Rossi[a,b], T. Rovelli[a,b], G. P. Siroli[a,b], N. Tosi[a]

INFN Sezione di Catania[a], Università di Catania[b], Catania, Italy
S. Albergo[a,b], A. Di Mattia[a], R. Potenza[a,b], A. Tricomi[a,b], C. Tuve[a,b]

INFN Sezione di Firenze[a], Università di Firenze[b], Firenze, Italy
G. Barbagli[a], K. Chatterjee[a,b], V. Ciulli[a,b], C. Civinini[a], R. D'Alessandro[a,b], E. Focardi[a,b], G. Latino, P. Lenzi[a,b], M. Meschini[a], S. Paoletti[a], L. Russo[a,28], G. Sguazzoni[a], D. Strom[a], L. Viliani[a]

INFN Laboratori Nazionali di Frascati, Frascati, Italy
L. Benussi, S. Bianco, F. Fabbri, D. Piccolo

INFN Sezione di Genova[a], Università di Genova[b], Genova, Italy
F. Ferro[a], R. Mulargia[a,b], E. Robutti[a], S. Tosi[a,b]

INFN Sezione di Milano-Bicocca[a], Università di Milano-Bicocca[b], Milano, Italy
A. Benaglia[a], A. Beschi[b], F. Brivio[a,b], V. Ciriolo[a,b,14], S. Di Guida[a,b,14], M. E. Dinardo[a,b], S. Fiorendi[a,b], S. Gennai[a], A. Ghezzi[a,b], P. Govoni[a,b], M. Malberti[a,b], S. Malvezzi[a], D. Menasce[a], F. Monti, L. Moroni[a], M. Paganoni[a,b], D. Pedrini[a], S. Ragazzi[a,b], T. Tabarelli de Fatis[a,b], D. Zuolo[a,b]

INFN Sezione di Napoli[a], Università di Napoli 'Federico II' [b], Napoli, Italy, Università della Basilicata[c], Potenza, Italy, Università G. Marconi[d], Roma, Italy
S. Buontempo[a], N. Cavallo[a,c], A. De Iorio[a,b], A. Di Crescenzo[a,b], F. Fabozzi[a,c], F. Fienga[a], G. Galati[a], A. O. M. Iorio[a,b], L. Lista[a], S. Meola[a,d,14], P. Paolucci[a,14], C. Sciacca[a,b], E. Voevodina[a,b]

INFN Sezione di Padova[a], Università di Padova[b], Padova, Italy, Università di Trento[c], Trento, Italy
P. Azzi[a], N. Bacchetta[a], D. Bisello[a,b], A. Boletti[a,b], A. Bragagnolo, R. Carlin[a,b], P. Checchia[a], M. Dall'Osso[a,b], P. De Castro Manzano[a], T. Dorigo[a], U. Dosselli[a], F. Gasparini[a,b], U. Gasparini[a,b], A. Gozzelino[a], S. Y. Hoh, S. Lacaprara[a], P. Lujan, M. Margoni[a,b], A. T. Meneguzzo[a,b], J. Pazzini[a], M. Presilla[b], P. Ronchese[a,b], R. Rossin[a,b], F. Simonetto[a,b], A. Tiko, E. Torassa[a], M. Tosi[a,b], M. Zanetti[a,b], P. Zotto[a,b], G. Zumerle[a,b]

INFN Sezione di Pavia[a], Università di Pavia[b], Pavia, Italy
A. Braghieri[a], A. Magnani[a], P. Montagna[a,b], S. P. Ratti[a,b], V. Re[a], M. Ressegotti[a,b], C. Riccardi[a,b], P. Salvini[a], I. Vai[a,b], P. Vitulo[a,b]

INFN Sezione di Perugia[a], Università di Perugia[b], Perugia, Italy
M. Biasini[a,b], G. M. Bilei[a], C. Cecchi[a,b], D. Ciangottini[a,b], L. Fanò[a,b], P. Lariccia[a,b], R. Leonardi[a,b], E. Manoni[a], G. Mantovani[a,b], V. Mariani[a,b], M. Menichelli[a], A. Rossi[a,b], A. Santocchia[a,b], D. Spiga[a]

INFN Sezione di Pisa[a], Università di Pisa[b], Scuola Normale Superiore di Pisa[c], Pisa, Italy
K. Androsov[a], P. Azzurri[a], G. Bagliesi[a], L. Bianchini[a], T. Boccali[a], L. Borrello, R. Castaldi[a], M. A. Ciocci[a,b], R. Dell'Orso[a], G. Fedi[a], F. Fiori[a,c], L. Giannini[a,c], A. Giassi[a], M. T. Grippo[a], F. Ligabue[a,c], E. Manca[a,c], G. Mandorli[a,c], A. Messineo[a,b], F. Palla[a], A. Rizzi[a,b], G. Rolandi[29], P. Spagnolo[a], R. Tenchini[a], G. Tonelli[a,b], A. Venturi[a], P. G. Verdini[a]

INFN Sezione di Roma[a], Sapienza Università di Roma[b], Rome, Italy
L. Barone[a,b], F. Cavallari[a], M. Cipriani[a,b], D. Del Re[a,b], E. Di Marco[a,b], M. Diemoz[a], S. Gelli[a,b], E. Longo[a,b], B. Marzocchi[a,b], P. Meridiani[a], G. Organtini[a,b], F. Pandolfi[a], R. Paramatti[a,b], F. Preiato[a,b], S. Rahatlou[a,b], C. Rovelli[a], F. Santanastasio[a,b]

INFN Sezione di Torino[a], Università di Torino[b], Torino, Italy, Università del Piemonte Orientale[c], Novara, Italy
N. Amapane[a,b], R. Arcidiacono[a,c], S. Argiro[a,b], M. Arneodo[a,c], N. Bartosik[a], R. Bellan[a,b], C. Biino[a], A. Cappati[a,b], N. Cartiglia[a], F. Cenna[a,b], S. Cometti[a], M. Costa[a,b], R. Covarelli[a,b], N. Demaria[a], B. Kiani[a,b], C. Mariotti[a], S. Maselli[a], E. Migliore[a,b], V. Monaco[a,b], E. Monteil[a,b], M. Monteno[a], M. M. Obertino[a,b], L. Pacher[a,b], N. Pastrone[a], M. Pelliccioni[a], G. L. Pinna Angioni[a,b], A. Romero[a,b], M. Ruspa[a,c], R. Sacchi[a,b], R. Salvatico[a,b], K. Shchelina[a,b], V. Sola[a], A. Solano[a,b], D. Soldi[a,b], A. Staiano[a]

INFN Sezione di Trieste[a], Università di Trieste[b], Trieste, Italy
S. Belforte[a], V. Candelise[a,b], M. Casarsa[a], F. Cossutti[a], A. Da Rold[a,b], G. Della Ricca[a,b], F. Vazzoler[a,b], A. Zanetti[a]

Kyungpook National University, Daegu, Korea
D. H. Kim, G. N. Kim, M. S. Kim, J. Lee, S. Lee, S. W. Lee, C. S. Moon, Y. D. Oh, S. I. Pak, S. Sekmen, D. C. Son, Y. C. Yang

Institute for Universe and Elementary Particles, Chonnam National University, Kwangju, Korea
H. Kim, D. H. Moon, G. Oh

Hanyang University, Seoul, Korea
B. Francois, J. Goh[30], T. J. Kim

Korea University, Seoul, Korea
S. Cho, S. Choi, Y. Go, D. Gyun, S. Ha, B. Hong, Y. Jo, K. Lee, K. S. Lee, S. Lee, J. Lim, S. K. Park, Y. Roh

Sejong University, Seoul, Korea
H. S. Kim

Seoul National University, Seoul, Korea
J. Almond, J. Kim, J. S. Kim, H. Lee, K. Lee, K. Nam, S. B. Oh, B. C. Radburn-Smith, S. h. Seo, U. K. Yang, H. D. Yoo, G. B. Yu

University of Seoul, Seoul, Korea
D. Jeon, H. Kim, J. H. Kim, J. S. H. Lee, I. C. Park

Sungkyunkwan University, Suwon, Korea
Y. Choi, C. Hwang, J. Lee, I. Yu

Riga Technical University, Riga, Latvia
V. Veckalns[31]

Vilnius University, Vilnius, Lithuania
V. Dudenas, A. Juodagalvis, J. Vaitkus

National Centre for Particle Physics, Universiti Malaya, Kuala Lumpur, Malaysia
Z. A. Ibrahim, M. A. B. Md Ali[32], F. Mohamad Idris[33], W. A. T. Wan Abdullah, M. N. Yusli, Z. Zolkapli

Universidad de Sonora (UNISON), Hermosillo, Mexico
J. F. Benitez, A. Castaneda Hernandez, J. A. Murillo Quijada

Centro de Investigacion y de Estudios Avanzados del IPN, Mexico City, Mexico
H. Castilla-Valdez, E. De La Cruz-Burelo, M. C. Duran-Osuna, I. Heredia-De La Cruz[34], R. Lopez-Fernandez, J. Mejia Guisao, R. I. Rabadan-Trejo, M. Ramirez-Garcia, G. Ramirez-Sanchez, R. Reyes-Almanza, A. Sanchez-Hernandez

Universidad Iberoamericana, Mexico City, Mexico
S. Carrillo Moreno, C. Oropeza Barrera, F. Vazquez Valencia

Benemerita Universidad Autonoma de Puebla, Puebla, Mexico
J. Eysermans, I. Pedraza, H. A. Salazar Ibarguen, C. Uribe Estrada

Universidad Autónoma de San Luis Potosí, San Luis Potosí, Mexico
A. Morelos Pineda

University of Auckland, Auckland, New Zealand
D. Krofcheck

University of Canterbury, Christchurch, New Zealand
S. Bheesette, P. H. Butler

National Centre for Physics, Quaid-I-Azam University, Islamabad, Pakistan
A. Ahmad, M. Ahmad, M. I. Asghar, Q. Hassan, H. R. Hoorani, W. A. Khan, M. A. Shah, M. Shoaib, M. Waqas

National Centre for Nuclear Research, Swierk, Poland
H. Bialkowska, M. Bluj, B. Boimska, T. Frueboes, M. Górski, M. Kazana, M. Szleper, P. Traczyk, P. Zalewski

Institute of Experimental Physics, Faculty of Physics, University of Warsaw, Warsaw, Poland
K. Bunkowski, A. Byszuk[35], K. Doroba, A. Kalinowski, M. Konecki, J. Krolikowski, M. Misiura, M. Olszewski, A. Pyskir, M. Walczak

Laboratório de Instrumentação e Física Experimental de Partículas, Lisboa, Portugal
M. Araujo, P. Bargassa, C. Beirão Da Cruz E Silva, A. Di Francesco, P. Faccioli, B. Galinhas, M. Gallinaro, J. Hollar, N. Leonardo, J. Seixas, G. Strong, O. Toldaiev, J. Varela

Joint Institute for Nuclear Research, Dubna, Russia
S. Afanasiev, P. Bunin, M. Gavrilenko, I. Golutvin, I. Gorbunov, A. Kamenev, V. Karjavine, A. Lanev, A. Malakhov, V. Matveev[36,37], P. Moisenz, V. Palichik, V. Perelygin, S. Shmatov, S. Shulha, N. Skatchkov, V. Smirnov, N. Voytishin, A. Zarubin

Petersburg Nuclear Physics Institute, Gatchina (St. Petersburg), Russia
V. Golovtsov, Y. Ivanov, V. Kim[38], E. Kuznetsova[39], P. Levchenko, V. Murzin, V. Oreshkin, I. Smirnov, D. Sosnov, V. Sulimov, L. Uvarov, S. Vavilov, A. Vorobyev

Institute for Nuclear Research, Moscow, Russia
Yu. Andreev, A. Dermenev, S. Gninenko, N. Golubev, A. Karneyeu, M. Kirsanov, N. Krasnikov, A. Pashenkov, A. Shabanov, D. Tlisov, A. Toropin

Institute for Theoretical and Experimental Physics, Moscow, Russia
V. Epshteyn, V. Gavrilov, N. Lychkovskaya, V. Popov, I. Pozdnyakov, G. Safronov, A. Spiridonov, A. Stepennov, V. Stolin, M. Toms, E. Vlasov, A. Zhokin

Moscow Institute of Physics and Technology, Moscow, Russia
T. Aushev

National Research Nuclear University 'Moscow Engineering Physics Institute' (MEPhI), Moscow, Russia
R. Chistov[40], M. Danilov[40], D. Philippov, E. Tarkovskii

P.N. Lebedev Physical Institute, Moscow, Russia
V. Andreev, M. Azarkin, I. Dremin[37], M. Kirakosyan, A. Terkulov

Skobeltsyn Institute of Nuclear Physics, Lomonosov Moscow State University, Moscow, Russia
A. Baskakov, A. Belyaev, E. Boos, V. Bunichev, M. Dubinin[41], L. Dudko, V. Klyukhin, O. Kodolova, N. Korneeva, I. Lokhtin, S. Obraztsov, M. Perfilov, V. Savrin

Novosibirsk State University (NSU), Novosibirsk, Russia
A. Barnyakov[42], V. Blinov[42], T. Dimova[42], L. Kardapoltsev[42], Y. Skovpen[42]

Institute for High Energy Physics of National Research Centre 'Kurchatov Institute', Protvino, Russia
I. Azhgirey, I. Bayshev, S. Bitioukov, V. Kachanov, A. Kalinin, D. Konstantinov, P. Mandrik, V. Petrov, R. Ryutin, S. Slabospitskii, A. Sobol, S. Troshin, N. Tyurin, A. Uzunian, A. Volkov

National Research Tomsk Polytechnic University, Tomsk, Russia
A. Babaev, S. Baidali, V. Okhotnikov

Faculty of Physics and Vinca Institute of Nuclear Sciences, University of Belgrade, Belgrade, Serbia
P. Adzic[43], P. Cirkovic, D. Devetak, M. Dordevic, P. Milenovic[44], J. Milosevic

Centro de Investigaciones Energéticas Medioambientales y Tecnológicas (CIEMAT), Madrid, Spain
J. Alcaraz Maestre, A. Álvarez Fernández, I. Bachiller, M. Barrio Luna, J. A. Brochero Cifuentes, M. Cerrada, N. Colino, B. De La Cruz, A. Delgado Peris, C. Fernandez Bedoya, J. P. Fernández Ramos, J. Flix, M. C. Fouz, O. Gonzalez Lopez, S. Goy Lopez, J. M. Hernandez, M. I. Josa, D. Moran, A. Pérez-Calero Yzquierdo, J. Puerta Pelayo, I. Redondo, L. Romero, S. Sánchez Navas, M. S. Soares, A. Triossi

Universidad Autónoma de Madrid, Madrid, Spain
C. Albajar, J. F. de Trocóniz

Universidad de Oviedo, Oviedo, Spain
J. Cuevas, C. Erice, J. Fernandez Menendez, S. Folgueras, I. Gonzalez Caballero, J. R. González Fernández, E. Palencia Cortezon, V. Rodríguez Bouza, S. Sanchez Cruz, J. M. Vizan Garcia

Instituto de Física de Cantabria (IFCA), CSIC-Universidad de Cantabria, Santander, Spain
I. J. Cabrillo, A. Calderon, B. Chazin Quero, J. Duarte Campderros, M. Fernandez, P. J. Fernández Manteca, A. García Alonso, J. Garcia-Ferrero, G. Gomez, A. Lopez Virto, J. Marco, C. Martinez Rivero, P. Martinez Ruiz del Arbol, F. Matorras, J. Piedra Gomez, C. Prieels, T. Rodrigo, A. Ruiz-Jimeno, L. Scodellaro, N. Trevisani, I. Vila, R. Vilar Cortabitarte

Department of Physics, University of Ruhuna, Matara, Sri Lanka
N. Wickramage

CERN, European Organization for Nuclear Research, Geneva, Switzerland
D. Abbaneo, B. Akgun, E. Auffray, G. Auzinger, P. Baillon, A. H. Ball, D. Barney, J. Bendavid, M. Bianco, A. Bocci, C. Botta, E. Brondolin, T. Camporesi, M. Cepeda, G. Cerminara, E. Chapon, Y. Chen, G. Cucciati, D. d'Enterria, A. Dabrowski, N. Daci, V. Daponte, A. David, A. De Roeck, N. Deelen, M. Dobson, M. Dünser, N. Dupont, A. Elliott-Peisert, F. Fallavollita[45], D. Fasanella, G. Franzoni, J. Fulcher, W. Funk, D. Gigi, A. Gilbert, K. Gill, F. Glege, M. Gruchala, M. Guilbaud, D. Gulhan, J. Hegeman, C. Heidegger, V. Innocente, G. M. Innocenti, A. Jafari, P. Janot, O. Karacheban[17], J. Kieseler, A. Kornmayer, M. Krammer[1], C. Lange, P. Lecoq, C. Lourenço, L. Malgeri, M. Mannelli, A. Massironi, F. Meijers, J. A. Merlin, S. Mersi, E. Meschi, F. Moortgat, M. Mulders, J. Ngadiuba, S. Nourbakhsh, S. Orfanelli, L. Orsini, F. Pantaleo[14], L. Pape, E. Perez, M. Peruzzi, A. Petrilli, G. Petrucciani, A. Pfeiffer, M. Pierini, F. M. Pitters, D. Rabady, A. Racz, T. Reis, M. Rovere, H. Sakulin, C. Schäfer, C. Schwick, M. Selvaggi, A. Sharma, P. Silva, P. Sphicas[46], A. Stakia, J. Steggemann, D. Treille, A. Tsirou, A. Vartak, M. Verzetti, W. D. Zeuner

Paul Scherrer Institut, Villigen, Switzerland
L. Caminada[47], K. Deiters, W. Erdmann, R. Horisberger, Q. Ingram, H. C. Kaestli, D. Kotlinski, U. Langenegger, T. Rohe, S. A. Wiederkehr

ETH Zurich-Institute for Particle Physics and Astrophysics (IPA), Zurich, Switzerland
M. Backhaus, L. Bäni, P. Berger, N. Chernyavskaya, G. Dissertori, M. Dittmar, M. Donegà, C. Dorfer, T. A. Gómez Espinosa, C. Grab, D. Hits, T. Klijnsma, W. Lustermann, R. A. Manzoni, M. Marionneau, M. T. Meinhard, F. Micheli, P. Musella, F. Nessi-Tedaldi, F. Pauss, G. Perrin, L. Perrozzi, S. Pigazzini, M. Reichmann, C. Reissel, D. Ruini, D. A. Sanz Becerra, M. Schönenberger, L. Shchutska, V. R. Tavolaro, K. Theofilatos, M. L. Vesterbacka Olsson, R. Wallny, D. H. Zhu

Universität Zürich, Zurich, Switzerland
T. K. Aarrestad, C. Amsler[48], D. Brzhechko, M. F. Canelli, A. De Cosa, R. Del Burgo, S. Donato, C. Galloni, T. Hreus, B. Kilminster, S. Leontsinis, I. Neutelings, G. Rauco, P. Robmann, D. Salerno, K. Schweiger, C. Seitz, Y. Takahashi, S. Wertz, A. Zucchetta

National Central University, Chung-Li, Taiwan
T. H. Doan, R. Khurana, C. M. Kuo, W. Lin, A. Pozdnyakov, S. S. Yu

National Taiwan University (NTU), Taipei, Taiwan
P. Chang, Y. Chao, K. F. Chen, P. H. Chen, W.-S. Hou, Y. F. Liu, R.-S. Lu, E. Paganis, A. Psallidas, A. Steen

Department of Physics, Faculty of Science, Chulalongkorn University, Bangkok, Thailand
B. Asavapibhop, N. Srimanobhas, N. Suwonjandee

Physics Department, Science and Art Faculty, Çukurova University, Adana, Turkey
A. Bat, F. Boran, S. Cerci[49], S. Damarseckin, Z. S. Demiroglu, F. Dolek, C. Dozen, I. Dumanoglu, G. Gokbulut, Y. Guler, E. Gurpinar, I. Hos[50], C. Isik, E. E. Kangal[51], O. Kara, A. Kayis Topaksu, U. Kiminsu, M. Oglakci, G. Onengut, K. Ozdemir[52], S. Ozturk[53], D. Sunar Cerci[49], B. Tali[49], U. G. Tok, S. Turkcapar, I. S. Zorbakir, C. Zorbilmez

Physics Department, Middle East Technical University, Ankara, Turkey
B. Isildak[54], G. Karapinar[55], M. Yalvac, M. Zeyrek

Bogazici University, Istanbul, Turkey
I. O. Atakisi, E. Gülmez, M. Kaya[56], O. Kaya[57], S. Ozkorucuklu[58], S. Tekten, E. A. Yetkin[59]

Istanbul Technical University, Istanbul, Turkey
M. N. Agaras, A. Cakir, K. Cankocak, Y. Komurcu, S. Sen[60]

Institute for Scintillation Materials of National Academy of Science of Ukraine, Kharkov, Ukraine
B. Grynyov

National Scientific Center, Kharkov Institute of Physics and Technology, Kharkov, Ukraine
L. Levchuk

University of Bristol, Bristol, UK
F. Ball, J. J. Brooke, D. Burns, E. Clement, D. Cussans, O. Davignon, H. Flacher, J. Goldstein, G. P. Heath, H. F. Heath, L. Kreczko, D. M. Newbold[61], S. Paramesvaran, B. Penning, T. Sakuma, D. Smith, V. J. Smith, J. Taylor, A. Titterton

Rutherford Appleton Laboratory, Didcot, UK
K. W. Bell, A. Belyaev[62], C. Brew, R. M. Brown, D. Cieri, D. J. A. Cockerill, J. A. Coughlan, K. Harder, S. Harper, J. Linacre, K. Manolopoulos, E. Olaiya, D. Petyt, T. Schuh, C. H. Shepherd-Themistocleous, A. Thea, I. R. Tomalin, T. Williams, W. J. Womersley

Imperial College, London, UK
R. Bainbridge, P. Bloch, J. Borg, S. Breeze, O. Buchmuller, A. Bundock, D. Colling, P. Dauncey, G. Davies, M. Della Negra, R. Di Maria, P. Everaerts, G. Hall, G. Iles, T. James, M. Komm, C. Laner, L. Lyons, A.-M. Magnan, S. Malik, A. Martelli, J. Nash[63], A. Nikitenko[7], V. Palladino, M. Pesaresi, D. M. Raymond, A. Richards, A. Rose, E. Scott, C. Seez, A. Shtipliyski, G. Singh, M. Stoye, T. Strebler, S. Summers, A. Tapper, K. Uchida, T. Virdee[14], N. Wardle, D. Winterbottom, J. Wright, S. C. Zenz

Brunel University, Uxbridge, UK
J. E. Cole, P. R. Hobson, A. Khan, P. Kyberd, C. K. Mackay, A. Morton, I. D. Reid, L. Teodorescu, S. Zahid

Baylor University, Waco, USA
K. Call, J. Dittmann, K. Hatakeyama, H. Liu, C. Madrid, B. McMaster, N. Pastika, C. Smith

Catholic University of America, Washington DC, USA
R. Bartek, A. Dominguez

The University of Alabama, Tuscaloosa, USA
A. Buccilli, S. I. Cooper, C. Henderson, P. Rumerio, C. West

Boston University, Boston, USA
D. Arcaro, T. Bose, D. Gastler, S. Girgis, D. Pinna, C. Richardson, J. Rohlf, L. Sulak, D. Zou

Brown University, Providence, USA
G. Benelli, B. Burkle, X. Coubez, D. Cutts, M. Hadley, J. Hakala, U. Heintz, J. M. Hogan[64], K. H. M. Kwok, E. Laird, G. Landsberg, J. Lee, Z. Mao, M. Narain, S. Sagir[65], R. Syarif, E. Usai, D. Yu

University of California, Davis, Davis, USA
R. Band, C. Brainerd, R. Breedon, D. Burns, M. Calderon De La Barca Sanchez, M. Chertok, J. Conway, R. Conway, P. T. Cox, R. Erbacher, C. Flores, G. Funk, W. Ko, O. Kukral, R. Lander, M. Mulhearn, D. Pellett, J. Pilot, S. Shalhout, M. Shi, D. Stolp, D. Taylor, K. Tos, M. Tripathi, Z. Wang, F. Zhang

University of California, Los Angeles, USA
M. Bachtis, C. Bravo, R. Cousins, A. Dasgupta, S. Erhan, A. Florent, J. Hauser, M. Ignatenko, N. Mccoll, S. Regnard, D. Saltzberg, C. Schnaible, V. Valuev

University of California, Riverside, Riverside, USA
E. Bouvier, K. Burt, R. Clare, J. W. Gary, S. M. A. Ghiasi Shirazi, G. Hanson, G. Karapostoli, E. Kennedy, F. Lacroix, O. R. Long, M. Olmedo Negrete, M. I. Paneva, W. Si, L. Wang, H. Wei, S. Wimpenny, B. R. Yates

University of California, San Diego, La Jolla, USA
J. G. Branson, P. Chang, S. Cittolin, M. Derdzinski, R. Gerosa, D. Gilbert, B. Hashemi, A. Holzner, D. Klein, G. Kole, V. Krutelyov, J. Letts, M. Masciovecchio, S. May, D. Olivito, S. Padhi, M. Pieri, V. Sharma, M. Tadel, J. Wood, F. Würthwein, A. Yagil, G. Zevi Della Porta

Department of Physics, University of California, Santa Barbara, Santa Barbara, USA
N. Amin, R. Bhandari, C. Campagnari, M. Citron, V. Dutta, M. Franco Sevilla, L. Gouskos, R. Heller, J. Incandela, H. Mei, A. Ovcharova, H. Qu, J. Richman, D. Stuart, I. Suarez, S. Wang, J. Yoo

California Institute of Technology, Pasadena, USA
D. Anderson, A. Bornheim, J. M. Lawhorn, N. Lu, H. B. Newman, T. Q. Nguyen, J. Pata, M. Spiropulu, J. R. Vlimant, R. Wilkinson, S. Xie, Z. Zhang, R. Y. Zhu

Carnegie Mellon University, Pittsburgh, USA
M. B. Andrews, T. Ferguson, T. Mudholkar, M. Paulini, M. Sun, I. Vorobiev, M. Weinberg

University of Colorado Boulder, Boulder, USA
J. P. Cumalat, W. T. Ford, F. Jensen, A. Johnson, E. MacDonald, T. Mulholland, R. Patel, A. Perloff, K. Stenson, K. A. Ulmer, S. R. Wagner

Cornell University, Ithaca, USA
J. Alexander, J. Chaves, Y. Cheng, J. Chu, A. Datta, K. Mcdermott, N. Mirman, J. R. Patterson, D. Quach, A. Rinkevicius, A. Ryd, L. Skinnari, L. Soffi, S. M. Tan, Z. Tao, J. Thom, J. Tucker, P. Wittich, M. Zientek

Fermi National Accelerator Laboratory, Batavia, USA
S. Abdullin, M. Albrow, M. Alyari, G. Apollinari, A. Apresyan, A. Apyan, S. Banerjee, L. A. T. Bauerdick, A. Beretvas, J. Berryhill, P. C. Bhat, K. Burkett, J. N. Butler, A. Canepa, G. B. Cerati, H. W. K. Cheung, F. Chlebana, M. Cremonesi, J. Duarte, V. D. Elvira, J. Freeman, Z. Gecse, E. Gottschalk, L. Gray, D. Green, S. Grünendahl, O. Gutsche, J. Hanlon, R. M. Harris, S. Hasegawa, J. Hirschauer, Z. Hu, B. Jayatilaka, S. Jindariani, M. Johnson, U. Joshi, B. Klima, M. J. Kortelainen, B. Kreis, S. Lammel, D. Lincoln, R. Lipton, M. Liu, T. Liu, J. Lykken, K. Maeshima, J. M. Marraffino, D. Mason, P. McBride, P. Merkel, S. Mrenna, S. Nahn, V. O'Dell, K. Pedro, C. Pena, O. Prokofyev, G. Rakness, F. Ravera, A. Reinsvold, L. Ristori, A. Savoy-Navarro[66], B. Schneider, E. Sexton-Kennedy, A. Soha, W. J. Spalding, L. Spiegel, S. Stoynev, J. Strait, N. Strobbe, L. Taylor, S. Tkaczyk, N. V. Tran, L. Uplegger, E. W. Vaandering, C. Vernieri, M. Verzocchi, R. Vidal, M. Wang, H. A. Weber

University of Florida, Gainesville, USA
D. Acosta, P. Avery, P. Bortignon, D. Bourilkov, A. Brinkerhoff, L. Cadamuro, A. Carnes, D. Curry, R. D. Field, S. V. Gleyzer, B. M. Joshi, J. Konigsberg, A. Korytov, K. H. Lo, P. Ma, K. Matchev, N. Menendez, G. Mitselmakher, D. Rosenzweig, K. Shi, D. Sperka, J. Wang, S. Wang, X. Zuo

Florida International University, Miami, USA
Y. R. Joshi, S. Linn

Florida State University, Tallahassee, USA
A. Ackert, T. Adams, A. Askew, S. Hagopian, V. Hagopian, K. F. Johnson, T. Kolberg, G. Martinez, T. Perry, H. Prosper, A. Saha, C. Schiber, R. Yohay

Florida Institute of Technology, Melbourne, USA
M. M. Baarmand, V. Bhopatkar, S. Colafranceschi, M. Hohlmann, D. Noonan, M. Rahmani, T. Roy, M. Saunders, F. Yumiceva

University of Illinois at Chicago (UIC), Chicago, USA
M. R. Adams, L. Apanasevich, D. Berry, R. R. Betts, R. Cavanaugh, X. Chen, S. Dittmer, O. Evdokimov, C. E. Gerber, D. A. Hangal, D. J. Hofman, K. Jung, J. Kamin, C. Mills, M. B. Tonjes, N. Varelas, H. Wang, X. Wang, Z. Wu, J. Zhang

The University of Iowa, Iowa City, USA
M. Alhusseini, B. Bilki[67], W. Clarida, K. Dilsiz[68], S. Durgut, R. P. Gandrajula, M. Haytmyradov, V. Khristenko, J.-P. Merlo, A. Mestvirishvili, A. Moeller, J. Nachtman, H. Ogul[69], Y. Onel, F. Ozok[70], A. Penzo, C. Snyder, E. Tiras, J. Wetzel

Johns Hopkins University, Baltimore, USA
B. Blumenfeld, A. Cocoros, N. Eminizer, D. Fehling, L. Feng, A. V. Gritsan, W. T. Hung, P. Maksimovic, J. Roskes, U. Sarica, M. Swartz, M. Xiao

The University of Kansas, Lawrence, USA
A. Al-bataineh, P. Baringer, A. Bean, S. Boren, J. Bowen, A. Bylinkin, J. Castle, S. Khalil, A. Kropivnitskaya, D. Majumder, W. Mcbrayer, M. Murray, C. Rogan, S. Sanders, E. Schmitz, J. D. Tapia Takaki, Q. Wang

Kansas State University, Manhattan, USA
S. Duric, A. Ivanov, K. Kaadze, D. Kim, Y. Maravin, D. R. Mendis, T. Mitchell, A. Modak, A. Mohammadi

Lawrence Livermore National Laboratory, Livermore, USA
F. Rebassoo, D. Wright

University of Maryland, College Park, USA
A. Baden, O. Baron, A. Belloni, S. C. Eno, Y. Feng, C. Ferraioli, N. J. Hadley, S. Jabeen, G. Y. Jeng, R. G. Kellogg, J. Kunkle, A. C. Mignerey, S. Nabili, F. Ricci-Tam, M. Seidel, Y. H. Shin, A. Skuja, S. C. Tonwar, K. Wong

Massachusetts Institute of Technology, Cambridge, USA
D. Abercrombie, B. Allen, V. Azzolini, A. Baty, R. Bi, S. Brandt, W. Busza, I. A. Cali, M. D'Alfonso, Z. Demiragli, G. Gomez Ceballos, M. Goncharov, P. Harris, D. Hsu, M. Hu, Y. Iiyama, M. Klute, D. Kovalskyi, Y.-J. Lee, P. D. Luckey, B. Maier, A. C. Marini, C. Mcginn, C. Mironov, S. Narayanan, X. Niu, C. Paus, D. Rankin, C. Roland, G. Roland, Z. Shi, G. S. F. Stephans, K. Sumorok, K. Tatar, D. Velicanu, J. Wang, T. W. Wang, B. Wyslouch

University of Minnesota, Minneapolis, USA
A. C. Benvenuti[†], R. M. Chatterjee, A. Evans, P. Hansen, J. Hiltbrand, Sh. Jain, S. Kalafut, M. Krohn, Y. Kubota, Z. Lesko, J. Mans, R. Rusack, M. A. Wadud

University of Mississippi, Oxford, USA
J. G. Acosta, S. Oliveros

University of Nebraska-Lincoln, Lincoln, USA
E. Avdeeva, K. Bloom, D. R. Claes, C. Fangmeier, F. Golf, R. Gonzalez Suarez, R. Kamalieddin, I. Kravchenko, J. Monroy, J. E. Siado, G. R. Snow, B. Stieger

State University of New York at Buffalo, Buffalo, USA
A. Godshalk, C. Harrington, I. Iashvili, A. Kharchilava, C. Mclean, D. Nguyen, A. Parker, S. Rappoccio, B. Roozbahani

Northeastern University, Boston, USA
G. Alverson, E. Barberis, C. Freer, Y. Haddad, A. Hortiangtham, G. Madigan, D. M. Morse, T. Orimoto, A. Tishelman-charny, T. Wamorkar, B. Wang, A. Wisecarver, D. Wood

Northwestern University, Evanston, USA
S. Bhattacharya, J. Bueghly, O. Charaf, T. Gunter, K. A. Hahn, N. Odell, M. H. Schmitt, K. Sung, M. Trovato, M. Velasco

University of Notre Dame, Notre Dame, USA
R. Bucci, N. Dev, R. Goldouzian, M. Hildreth, K. Hurtado Anampa, C. Jessop, D. J. Karmgard, K. Lannon, W. Li, N. Loukas, N. Marinelli, F. Meng, C. Mueller, Y. Musienko[36], M. Planer, R. Ruchti, P. Siddireddy, G. Smith, S. Taroni, M. Wayne, A. Wightman, M. Wolf, A. Woodard

The Ohio State University, Columbus, USA
J. Alimena, L. Antonelli, B. Bylsma, L. S. Durkin, S. Flowers, B. Francis, C. Hill, W. Ji, T. Y. Ling, W. Luo, B. L. Winer

Princeton University, Princeton, USA
S. Cooperstein, P. Elmer, J. Hardenbrook, N. Haubrich, S. Higginbotham, A. Kalogeropoulos, S. Kwan, D. Lange, M. T. Lucchini, J. Luo, D. Marlow, K. Mei, I. Ojalvo, J. Olsen, C. Palmer, P. Piroué, J. Salfeld-Nebgen, D. Stickland, C. Tully

University of Puerto Rico, Mayaguez, USA
S. Malik, S. Norberg

Purdue University, West Lafayette, USA
A. Barker, V. E. Barnes, S. Das, L. Gutay, M. Jones, A. W. Jung, A. Khatiwada, B. Mahakud, D. H. Miller, N. Neumeister, C. C. Peng, S. Piperov, H. Qiu, J. F. Schulte, J. Sun, F. Wang, R. Xiao, W. Xie

Purdue University Northwest, Hammond, USA
T. Cheng, J. Dolen, N. Parashar

Rice University, Houston, USA
Z. Chen, K. M. Ecklund, S. Freed, F. J. M. Geurts, M. Kilpatrick, Arun Kumar, W. Li, B. P. Padley, R. Redjimi, J. Roberts, J. Rorie, W. Shi, Z. Tu, A. Zhang

University of Rochester, Rochester, USA
A. Bodek, P. de Barbaro, R. Demina, Y. t. Duh, J. L. Dulemba, C. Fallon, T. Ferbel, M. Galanti, A. Garcia-Bellido, J. Han, O. Hindrichs, A. Khukhunaishvili, E. Ranken, P. Tan, R. Taus

Rutgers, The State University of New Jersey, Piscataway, USA
B. Chiarito, J. P. Chou, Y. Gershtein, E. Halkiadakis, A. Hart, M. Heindl, E. Hughes, S. Kaplan, R. Kunnawalkam Elayavalli, S. Kyriacou, I. Laflotte, A. Lath, R. Montalvo, K. Nash, M. Osherson, H. Saka, S. Salur, S. Schnetzer, D. Sheffield, S. Somalwar, R. Stone, S. Thomas, P. Thomassen

University of Tennessee, Knoxville, USA
H. Acharya, A. G. Delannoy, J. Heideman, G. Riley, S. Spanier

Texas A& M University, College Station, USA
O. Bouhali[71], A. Celik, M. Dalchenko, M. De Mattia, A. Delgado, S. Dildick, R. Eusebi, J. Gilmore, T. Huang, T. Kamon[72], S. Luo, D. Marley, R. Mueller, D. Overton, L. Perniè, D. Rathjens, A. Safonov

Texas Tech University, Lubbock, USA
N. Akchurin, J. Damgov, F. De Guio, P. R. Dudero, S. Kunori, K. Lamichhane, S. W. Lee, T. Mengke, S. Muthumuni, T. Peltola, S. Undleeb, I. Volobouev, Z. Wang, A. Whitbeck

Vanderbilt University, Nashville, USA
S. Greene, A. Gurrola, R. Janjam, W. Johns, C. Maguire, A. Melo, H. Ni, K. Padeken, F. Romeo, P. Sheldon, S. Tuo, J. Velkovska, M. Verweij, Q. Xu

University of Virginia, Charlottesville, USA
M. W. Arenton, P. Barria, B. Cox, R. Hirosky, M. Joyce, A. Ledovskoy, H. Li, C. Neu, T. Sinthuprasith, Y. Wang, E. Wolfe, F. Xia

Wayne State University, Detroit, USA
R. Harr, P. E. Karchin, N. Poudyal, J. Sturdy, P. Thapa, S. Zaleski

University of Wisconsin-Madison, Madison, WI, USA
J. Buchanan, C. Caillol, D. Carlsmith, S. Dasu, I. De Bruyn, L. Dodd, B. Gomber[73], M. Grothe, M. Herndon, A. Hervé, U. Hussain, P. Klabbers, A. Lanaro, K. Long, R. Loveless, T. Ruggles, A. Savin, V. Sharma, N. Smith, W. H. Smith, N. Woods

† **Deceased**

1: Also at Vienna University of Technology, Vienna, Austria
2: Also at IRFU, CEA, Université Paris-Saclay, Gif-sur-Yvette, France
3: Also at Universidade Estadual de Campinas, Campinas, Brazil
4: Also at Federal University of Rio Grande do Sul, Porto Alegre, Brazil
5: Also at Université Libre de Bruxelles, Bruxelles, Belgium
6: Also at University of Chinese Academy of Sciences, Beijing, China
7: Also at Institute for Theoretical and Experimental Physics, Moscow, Russia
8: Also at Joint Institute for Nuclear Research, Dubna, Russia
9: Also at Cairo University, Cairo, Egypt
10: Also at Zewail City of Science and Technology, Zewail, Egypt
11: Also at Department of Physics, King Abdulaziz University, Jeddah, Saudi Arabia
12: Also at Université de Haute Alsace, Mulhouse, France
13: Also at Skobeltsyn Institute of Nuclear Physics, Lomonosov Moscow State University, Moscow, Russia
14: Also at CERN, European Organization for Nuclear Research, Geneva, Switzerland
15: Also at RWTH Aachen University, III. Physikalisches Institut A, Aachen, Germany
16: Also at University of Hamburg, Hamburg, Germany
17: Also at Brandenburg University of Technology, Cottbus, Germany
18: Also at Institute of Physics, University of Debrecen, Debrecen, Hungary
19: Also at Institute of Nuclear Research ATOMKI, Debrecen, Hungary
20: Also at MTA-ELTE Lendület CMS Particle and Nuclear Physics Group, Eötvös Loránd University, Budapest, Hungary
21: Also at Indian Institute of Technology Bhubaneswar, Bhubaneswar, India
22: Also at Institute of Physics, Bhubaneswar, India
23: Also at Shoolini University, Solan, India
24: Also at University of Visva-Bharati, Santiniketan, India
25: Also at Isfahan University of Technology, Isfahan, Iran
26: Also at Plasma Physics Research Center, Science and Research Branch, Islamic Azad University, Tehran, Iran
27: Also at ITALIAN NATIONAL AGENCY FOR NEW TECHNOLOGIES, ENERGY AND SUSTAINABLE ECONOMIC DEVELOPMENT, Bologna, Italy
28: Also at Università degli Studi di Siena, Siena, Italy
29: Also at Scuola Normale e Sezione dell'INFN, Pisa, Italy
30: Also at Kyunghee University, Seoul, Korea
31: Also at Riga Technical University, Riga, Latvia
32: Also at International Islamic University of Malaysia, Kuala Lumpur, Malaysia
33: Also at Malaysian Nuclear Agency, MOSTI, Kajang, Malaysia
34: Also at Consejo Nacional de Ciencia y Tecnología, Mexico City, Mexico
35: Also at Warsaw University of Technology, Institute of Electronic Systems, Warsaw, Poland
36: Also at Institute for Nuclear Research, Moscow, Russia
37: Now at National Research Nuclear University 'Moscow Engineering Physics Institute' (MEPhI), Moscow, Russia
38: Also at St. Petersburg State Polytechnical University, St. Petersburg, Russia
39: Also at University of Florida, Gainesville, USA
40: Also at P.N. Lebedev Physical Institute, Moscow, Russia
41: Also at California Institute of Technology, Pasadena, USA
42: Also at Budker Institute of Nuclear Physics, Novosibirsk, Russia
43: Also at Faculty of Physics, University of Belgrade, Belgrade, Serbia
44: Also at University of Belgrade, Faculty of Physics and Vinca Institute of Nuclear Sciences, Belgrade, Serbia
45: Also at INFN Sezione di Pavia [a], Università di Pavia [b], Pavia, Italy
46: Also at National and Kapodistrian University of Athens, Athens, Greece

47: Also at Universität Zürich, Zurich, Switzerland
48: Also at Stefan Meyer Institute for Subatomic Physics (SMI), Vienna, Austria
49: Also at Adiyaman University, Adiyaman, Turkey
50: Also at Istanbul Aydin University, Istanbul, Turkey
51: Also at Mersin University, Mersin, Turkey
52: Also at Piri Reis University, Istanbul, Turkey
53: Also at Gaziosmanpasa University, Tokat, Turkey
54: Also at Ozyegin University, Istanbul, Turkey
55: Also at Izmir Institute of Technology, Izmir, Turkey
56: Also at Marmara University, Istanbul, Turkey
57: Also at Kafkas University, Kars, Turkey
58: Also at Istanbul University, Faculty of Science, Istanbul, Turkey
59: Also at Istanbul Bilgi University, Istanbul, Turkey
60: Also at Hacettepe University, Ankara, Turkey
61: Also at Rutherford Appleton Laboratory, Didcot, UK
62: Also at School of Physics and Astronomy, University of Southampton, Southampton, UK
63: Also at Monash University, Faculty of Science, Clayton, Australia
64: Also at Bethel University, St. Paul, USA
65: Also at Karamanoğlu Mehmetbey University, Karaman, Turkey
66: Also at Purdue University, West Lafayette, USA
67: Also at Beykent University, Istanbul, Turkey
68: Also at Bingol University, Bingol, Turkey
69: Also at Sinop University, Sinop, Turkey
70: Also at Mimar Sinan University, Istanbul, Istanbul, Turkey
71: Also at Texas A&M University at Qatar, Doha, Qatar
72: Also at Kyungpook National University, Daegu, Korea
73: Also at University of Hyderabad, Hyderabad, India